Seismicity and Seismic Hazard of Lesotho

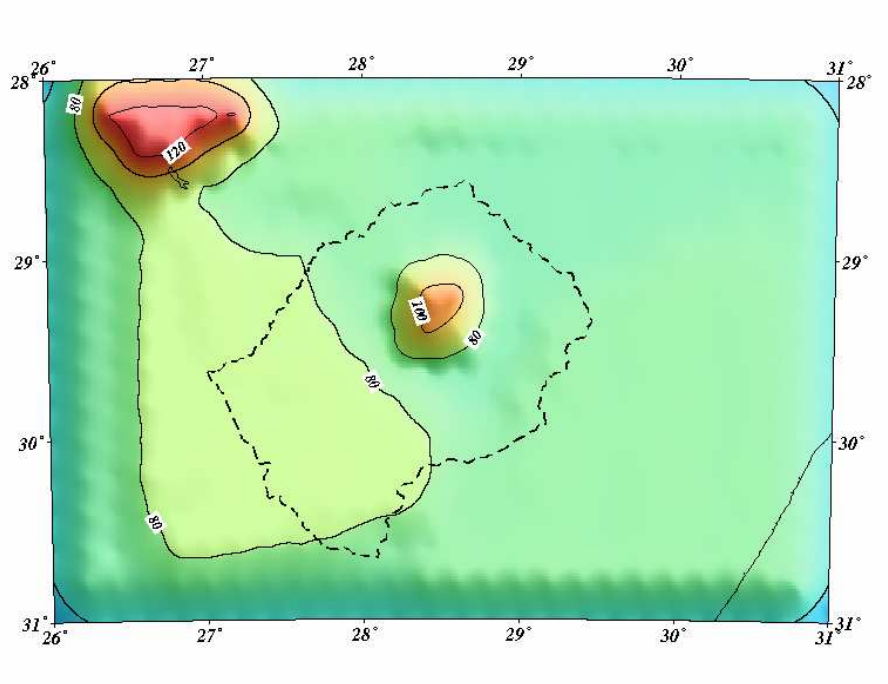

Hlompho R. Malephane

Faculty of Mathematics and Natural Sciences

Department of Earth Sciences

University of Bergen, Norway

November 2007

Abstract

Lesotho is a small country surrounded by South Africa and is characterized by a low level of intraplate seismicity which trends in a north-west to south-east direction. Recently scientists have identified this zone as a possible link to the extension of the East African Rift System into the Indian Ocean thereby forming a plate boundary. By use of data from three different agencies, a seismic catalogue for Lesotho is compiled and the seismicity is investigated. A probabilistic seismic hazard assessment is made based on the compiled catalogue. The results from this study indicate that the postulation of a boundary zone that accommodates the southward extension of the EARS is possible.

Table of Contents

1 Introduction

Earthquake distribution in space and time, as well as the associated seismic hazard in the country of Lesotho are difficult phenomena to understand. Situated on the stable continental interior of the African plate, Lesotho is characterized by a low level of intraplate seismicity, which may represent internal deformation of the plate. The central southern part of the country is characterized by a discrete zone of seismicity known as the Senqu Seismic Belt, which trends in a northwest-southeast direction and can be seen as part of the extension occurring along the East African Rift System (EARS) into the Indian Ocean (Hartnady, 2002). It is in this central southern part that two $M_L > 4.6$ earthquakes occurred within 20 minutes on January 27, 2002. Apart from minor landsides, no causalities or damages were reported as a result of these events. An $M_L = 5.1$ earthquake in 1986 occurred in the southern part of Lesotho and is the largest recorded within the country.

Intraplate earthquakes have longer recurrence times and higher stress drops than interplate earthquakes and their cause is difficult to understand (Kanamori and Anderson, 1975). Such earthquakes are often associated with extensional faulting deep within the continental crust where rifting is in its early stage (Stein and Wysession, 2003) In continental crust, faults remain close to their point of failure for longer parts of the earthquake cycle than at plate boundaries hence the long recurrence intervals for intraplate earthquakes (Hough et al., 2003). This means that stresses accumulate over long periods and therefore not released as frequently as is the case for plate boundaries. Examples of such earthquakes are seen in the series of events with magnitudes of up to $M_w = 8.0$, 1811 - 1812 New Madrid Fault, Missouri, (Johnston, 1996; Odum et al., 1998); intensity VIII 1886 Charleston, South Carolina (Hough et al., 2003; Musson, 2004) and the British Isles earthquakes

A major Mw = 7.0 earthquake in the southern African region, associated with the EARS occurred in the southern part of Mozambique on February 22, 2006. Mozambique is located at the southern end of the EARS and is generally considered a country with insignificant seismic hazard. This earthquake was felt throughout eastern Southern Africa but caused little damage (Fenton and Bommer, 2007). In the Ceres-Tulbach area in Cape Town, South Africa, a magnitude 6.3 earthquake, known to be the most destructive in modern South African history (Brandt, 2000), occurred on September 29, 1969 with an intensity VIII causing the loss of nine lives. In light of the above, it is likely that Lesotho can experience earthquakes of the same magnitude at any given time.

Besides information that is gathered from work done in the country of South Africa, no thorough seismicity study has been done for Lesotho as a country. Seismic monitoring in Lesotho was introduced by the implementation of the Lesotho Highlands Water Project (LHWP). The existing seismic network is located in the vicinity of the LHWP dams since it was designed for monitoring reservoir induced seismicity, however, it also serves as the country's network since there is no other. As a result of the main storage dam impoundment, induced earthquakes were triggered around the reservoir area with the largest of magnitude M_L = 3, occurring on January 3, 1996 some 5 km upstream of the dam wall, opening fresh fissures both along and transverse to an already existing shear zone (Brandt, 2000). The aim of this study is to document the seismicity of Lesotho - both natural and induced - by producing a reliable seismicity catalogue so as to better understand the earthquake occurrence and enable data integration to seismological agencies internationally.

In order to achieve this task, data from the local network has been re-analyzed and noise studies conducted in order to evaluate the validity of the data and network capability. A technical description of the local network as well as it operational statistics and data are given. Other data that is sourced from the International Seismological Center, UK and the Council for Geoscience, South Africa is also described. A seismic catalogue is produced and based on that, a preliminary probabilistic seismic hazard assessment is conducted.

2 Background tectonics and seismicity

The Kingdom of Lesotho is a small country with an area of about 32 000 km^2 and is completely surrounded by South Africa, rising from a plain at an altitude of about 1520 m in the west to over 3 350 m in the east (UNDP, 1984)The landscape of the country is in two major divisions, namely the lowlands and the highlands and is directly related to the underlying geology. The overall geological setting of Lesotho comprises horizontally layered sedimentary rocks overlain by basalt flows, which are intruded by dolerite dykes and sills. The highlands region is composed of sub-horizontal Jurassic basalts overlying the Karoo Basin sedimentary rocks, resting across a suture zone between the Archean Kaapvaal Craton and the Mezoproterozoic Namaqua-Natal orogenic belt (Hartnardy, 1998; James, 2003; James and Fouch, 2001; Mitha, 2006; UNDP, 1984).

In the following section the tectonics and seismicity are described on regional and local scales.

2.1 Tectonics

Though the African plate is known for its tectonically active East African Rift System (EARS), cratons and mobile belts characterize the southern part (Jacobs et al., 1993; Silver et al., 2001; Stein and Wysession, 2003), which is considered as not so active in terms of seismicity and tectonics.

Based on previous studies, the southern African region can be divided into 7 tectonic provinces namely, the Zimbabwe and Kaapvaal cratons; Limpopo mobile which formed as a result of the collision between Zimbabwe and Kaapvaal cratons, Kheis thrust belt, the Bushveld complex, all of which are of Archean origin; the Namaqua-Natal mobile

belt and the Cape fold belt which are younger than 2.0Ga (Silver et al., 2001). These mobile belts formed as a result of accretion during Proterozioc times and surround the cratons (James and Fouch, 2001). Figure 2.1 is a topographic map of Southern Africa showing these tectonic provinces.

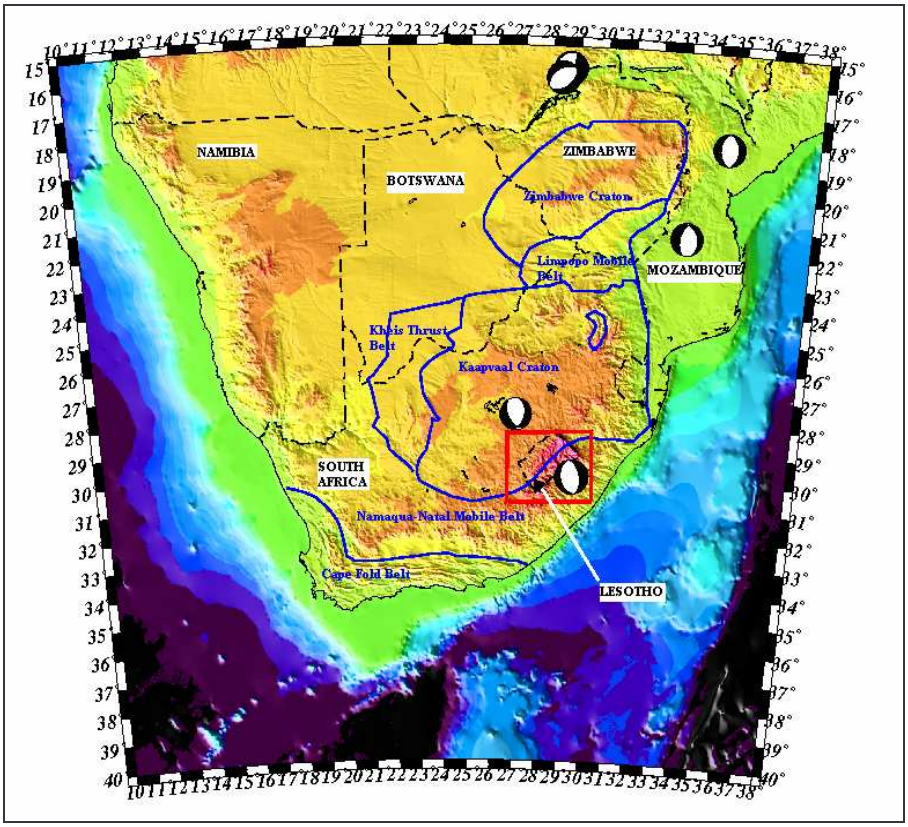

Figure 2.1: A topographic map of southern Africa showing the tectonic provinces and focal mechanisms from Havard Moment Tensor solutions. Note the boundary of the Kaapvaal Craton and Namaqua-Natal mobile belt cutting through Lesotho (in the red box). The provinces are modified from the South African Seismic Experiment Project (www.ciw.edu/Kaapvaal). The unlabelled part inside the Kaapvaal craton is part of the Bushveld complex.

The Kaapvaal Craton is characterized by numerous kimberlite pipes, one of which is found in the northern part of Lesotho (James et al., 2003; Mitha, 2006). The Namaqua-Natal mobile belt is characterized by northeast-southwest convergence (Jacobs and Thomas, 1994; Jacobs et al., 1993) and in the north of Lesotho it cuts through the kimberlite pipe.

Lesotho has the boundary between the Archean Kaapvaal craton and the subduction-related Namaqua-Natal Proterozoic orogenic belt traversing through from northeast to

southwest (Nguuri et al., 2001) as can be seen in figure 2.1. The Kaapvaal craton and the Namaqua-Natal mobile belt are considered the major tectonic provinces and together they form what is termed the Kalahari craton(Doucouré et al., 1996). In the context of the study area, these two are of great importance.

2.1.1. Regional tectonics

The African continent is situated on the relatively stable African plate, which is bounded, on the west by the mid-Atlantic ridge; in the south by the Antarctic ridge; to the east by the South West Indian Ridge (SWIR); to the north-east, by the Gulf of Aden/Afar triple junction and in the north by the Hellenic arc (subduction zone). As a result of the spreading due to the ridges, the African plate is relatively moving northwards where it collides with the Eurasian plate at the Hellenic arc and is being subducted. Figure 2.2 shows part of the African plate boundaries as modelled by (Bird, 2003).

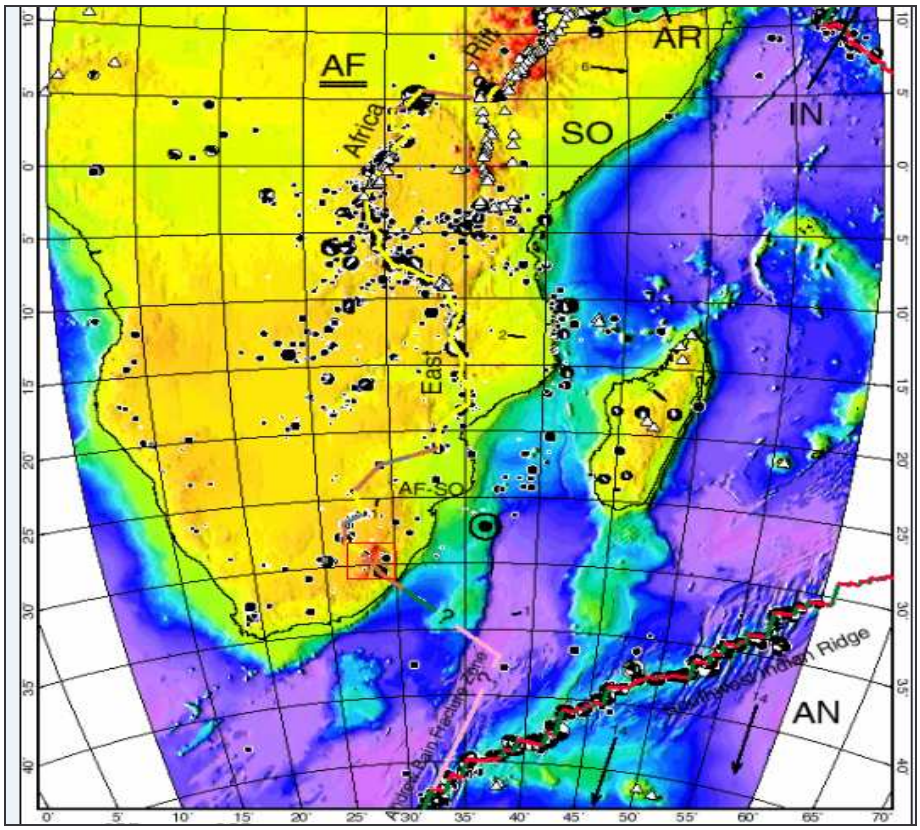

Figure 2.2: Tectonic map showing part of the African plate with boundaries as modelled by Bird (2003). The red square indicates the location of Lesotho.

In figure 2.2 AF refers to the African plate; SO to Somalian plate; AR to Arabian plate; IN to Indian plate and AN to Antarctica plate.

The African plate moves northwards at a relatively slow rate of 10 mm/yr (DeMets et al., 1990) while (McClusky et al., 2000) suggest this motion to be 5-6mm/yr compared to the Arabian and Euraisan plates that are moving at about 15mm/yr and 18-25mm/yr, respectively. This plate is considered one of the world's most stable regions in terms of tectonics. Within the continent, however, there is a spreading centre between the Nubian (west part) and Somalian (east part) plates with a slow rate of extension, commonly known as the East African Rift System (EARS), which has been noted from geological observations. The EARS is underlain by faults in the central part and cratons in the southern part. Seismicity within the rift ends in the southern part of Africa and while some scientists believe the extension connects to the South West Indian ridge (Bird, 2003; Hartnady, 2002; Rudolf, 2002; Rudolph, 2002), some believe the rift would not break the cratons, instead it would follow their boundaries(Stein and Wysession, 2003).

Several models have been developed to predict the movement of the Somalian plate, for example, Gordon (1995) suggests an eastward motion at a rate of about 3mm/yr while (Chu and Gordon, 1999) suggest 2mm/yr. Recent studies indicate that the Northern part of the rift is opening at a rate of 6mm/year while the southern part opens at about half that rate (Stein and Wysession, 2003) as the Euler pole is assumed to be in the south. As a result the southern extent of the rift is still a debatable matter, however, the Somalian plate is believed to be moving southeasterly relative to the Nubian plate (Horner-Johnson et al., 2005).

The East African Rift System is divided around lake Victoria, forming two branches, namely the Western branch of the East African Rift (WBR), which is marked by strong concave-east alignment of epicenters extending from southern Sudan through to Malawi; and the Eastern branch of the East Africa Rift (EBR), which is marked by a zone of more diffuse seismicity in Kenya & Tanzania extending offshore in Northern Mozambique (Fenton and Bommer, 2007).

2.1.2. Local Tectonics

The EARS in the southern part of Africa is not as clearly expressed as it is in the north. There are therefore ongoing efforts, such as the Southern African Seismic Experiment to understand the southern extent of the EARS. Furthermore, the plate boundary with the South West Indian Ridge is suggested to cross Lesotho (Bird, 2003; Gordon and Stein, 1992; Hartnady, 2002). See figure 2.2.

According to Hartnady (1998), Southern Africa is not "a coherent intraplate region but rather a wide boundary zone between the Nubian and Somalian plates, extending from EARS into Southern Africa with relatively aseismic blocks bounded by seismically more active seismic belts". A map of Lesotho showing the geological structures as well as the proposed plate boundary is seen in figure 2.3.

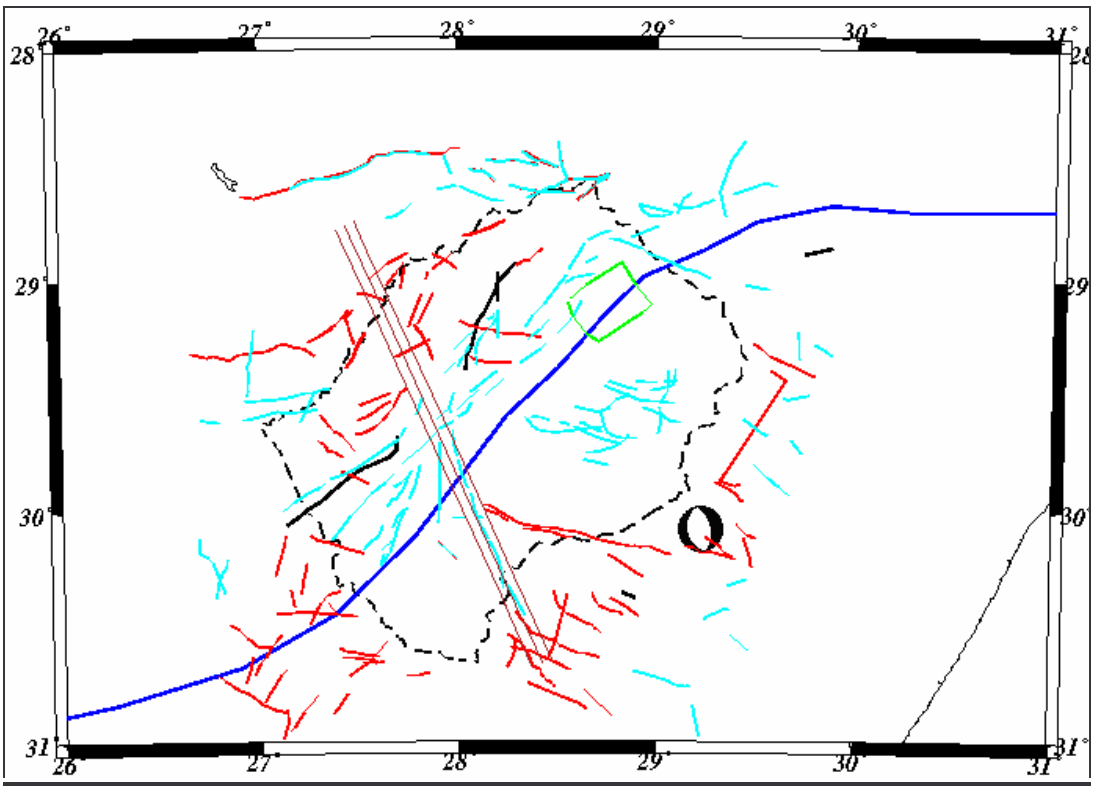

Figure 2.3: Map of Lesotho showing some geological structures and the proposed plate boundary (purple parallel lines); cyan lines indicate structural lineaments. Note that the proposed boundary follows one of the longest lineaments. Red lines indicate dolerite dykes; the green area is where the kimberlite pipes are located and the black lines indicate faults.The blue line is the Kaapvaal/Namaqua-natal boundary. Map modified from (Mellis and Chavellier, 2000).

2.2 Seismicity

Seismology in southern African has benefited greatly from the United States Geological Survey's (USGS) recent deployment of digital broadband stations as part of the Incorporated Research Institutes of Seismology (IRIS) plan for enhanced Global Seismographic Network (GSN). In this southern part of Africa, recent studies have shown the existence of two stable blocks from the distribution of earthquake epicentres. These are namely the Okavango rift in Botswana and the rift-grabens in Mozambique as well a discrete zone of seismicity across South Africa, between Namibia and Lesotho, known as the Senqu Seismic Belt (Hartnady, 2002). See figure 2.4.

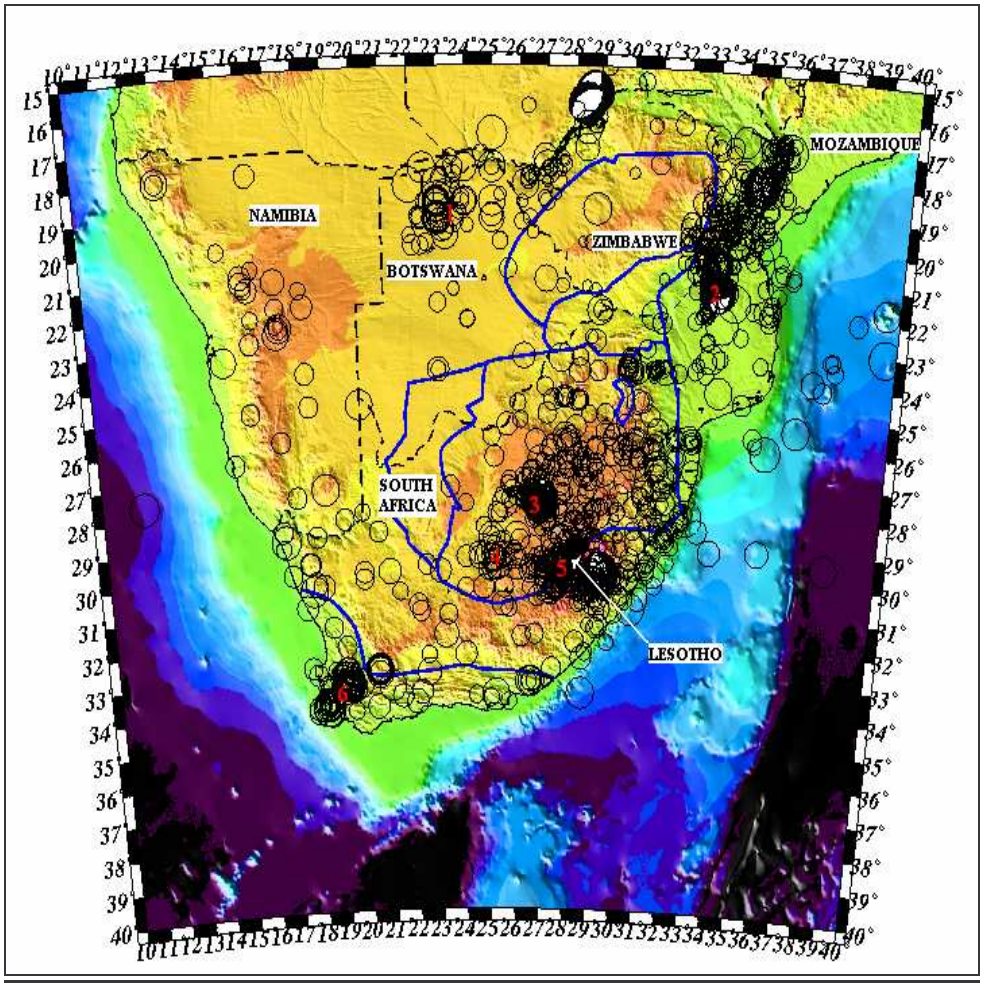

Figure 2.4: Earthquake distribution Map for Southern Africa for the period 1620 to 2006. The numbers in red denote the seismicity regions. Region 1 is the Okavango rift; region 2 is the Mozambique rift-grabens; region 3 represents the mines of South Africa; region 4 is the Koffiefontein cluster which together with region 5 in southern Lesotho, form the Senqu Seismic Belt; region 6 is the Ceres-Tulbagh region.

According to results from United States Geological Survey's Earthquake Hazard Program, the largest earthquake to have occurred in the EARS since the 20th century had a magnitude of about 7.6 and most of these earthquakes are either of normal or strike-slip faulting. A magnitude M_w = 7.0 earthquake occurred in Mozambique, in February 2006 and was felt throughout eastern southern Africa though causing little damage (Fenton and Bommer, 2007). The general east-west extension exhibited by known focal mechanisms in this region are in consistency with the stretching observed in the Mozambique channel (Bertil and Regnoult, 1998).

A map of epicentres, from the database created for this thesis, in figure 2.4 shows the distribution of earthquakes in southern Africa between 1620 and 2006.

2. 2. 1. Regional Seismicity

Seismic history in South Africa dates back to the year 1620. This historical information is complemented by the instrumental data recorded by the South African Seismic Network which began operation in 1910 (www.geoscience.org.za).

Natural seismic activity is considered low in Southern Africa and exhibits intraplate type of seismicity. The largest instrumentally recorded and documented earthquake with magnitude M_L = 6.3, was the most destructive in South African modern history, occurring on September 29, 1969 in the Ceres-Tulbagh area (Kijko et al., 2002). In Mozambique a magnitude Mw = 7.0 occurred on February 22, 2006 causing little damage though felt throughout southern Africa (Fenton and Bommer, 2007).

In southern Africa, the region which does not display characteristics of intraplate seismicity is considered a possible continuation of the EARS in the north eastern part with the narrow earthquake belt following the Mid-Atlantic ridge and Mid- Indian Ocean ridge.

Induced earthquakes also result from the deep mining activities in South Africa as well as reservoir induced activity from Lake Kariba, Zambia.

2.2.2. Local Seismicity

The region in which Lesotho lies is considered a possible example of a seismically active zone within an extensive lithospheric sector in a transition between a former stable continental region (SCR) and an incipient active continental region (ACR). A seismically active belt, trending West-North-West/East-South-East (WNW/ESE) across Lesotho propagates southwards from other belts of earthquake activity in southern Mozambique. This region is identified as the Senqu seismic belt and extends across South Africa, forming a southern boundary of a relatively aseismic block, which is lately identified as a possible "Trans-Gariep microplate" within the wide Somalia-Nubia plate boundary zone(Hartnardy, 1998). This belt includes the southern boundary of the Kaapvaal province, the Namaqua-Natal province, the Karoo basin and terminates in the Cape basin (Brandt, 2000). This region has a record of a magnitude M_b = 5.9 as the largest earthquake. The event occurred on July 1, 1976 in the Koffiefontein cluster see figure 2.5.

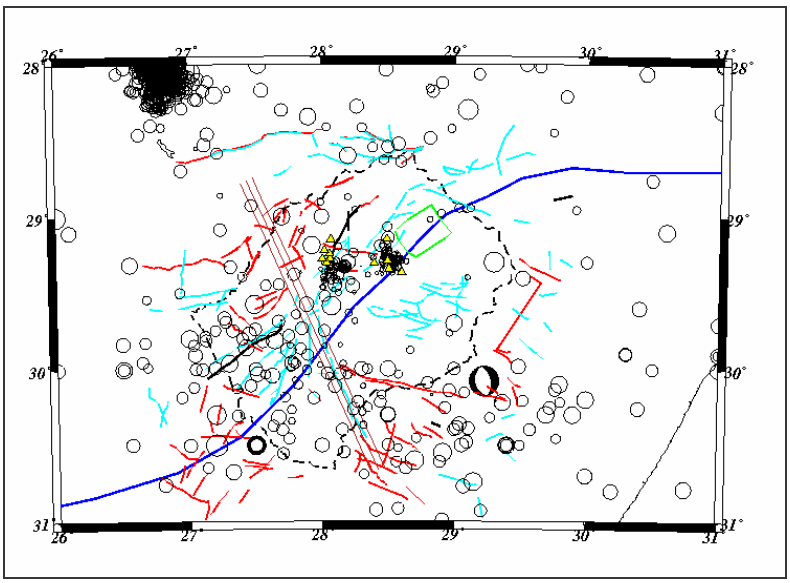

Figure 2.5: Seismicity map of Lesotho for the period 1620 to 2006. The earthquakes are transposed on the geological structures' map to illustrate their occurrence in relation to the proposed tectonic boundary. The earthquakes are marked by the black circles and the yellow triangles are the LHWP stations.The data is from Lesotho Highlands Water Project, Council for Geosceince and International Seismological Center.

Within the country, two magnitude 4.7 earthquakes were recorded 20 minutes apart on January 27, 2002, on the Senqu seismic belt. These are the largest instrumentally recorded events. From the earthquake catalogue compiled in this study, the first event within the borders of Lesotho had magnitude $M_L = 3.0$ in 1883. There have been several $M_L > 4.5$ events within the borders of Lesotho and the largest event has $M_L = 5.1$ located in the southern part in 1986. Figure 2.5 is a map of the distribution of earthquakes with reference to the proposed tectonic boundary.

Reservoir induced seismicity has been observed during the filling of the Katse dam under the Lesotho Highlands Water Project. The largest earthquake was recorded on January 3, 1996 some 5 km upstream of the main dam (Katse) with magnitude $M_b = 3.2$. From figure 2.5, it is obvious that seismicity of Lesotho is more in the southern part and it should be taken into account that the LHWP is located in the northern part of the country.

3 The Local Network and its Data

The bi-national Lesotho Highlands Water Project (LHWP) between Lesotho and South Africa is the most comprehensive engineering project in Southern Africa. Large dams are built in Lesotho for purposes of local electricity generation and water transfer to South Africa thereby providing revenue in the form of royalties. The LHWP is envisaged to be a 4-Phase project, of which only Phase 1 is complete and feasibility studies are currently ongoing for Phase 2. Phase 1 comprises the Katse dam, which is the main storage; 'Muela Hydro-power station, Mohale Dam and Matsoku diversion tunnel. Figure 3.1 shows the country of Lesotho and the LHWP region with highlights on Phase1 (complete part of the project).

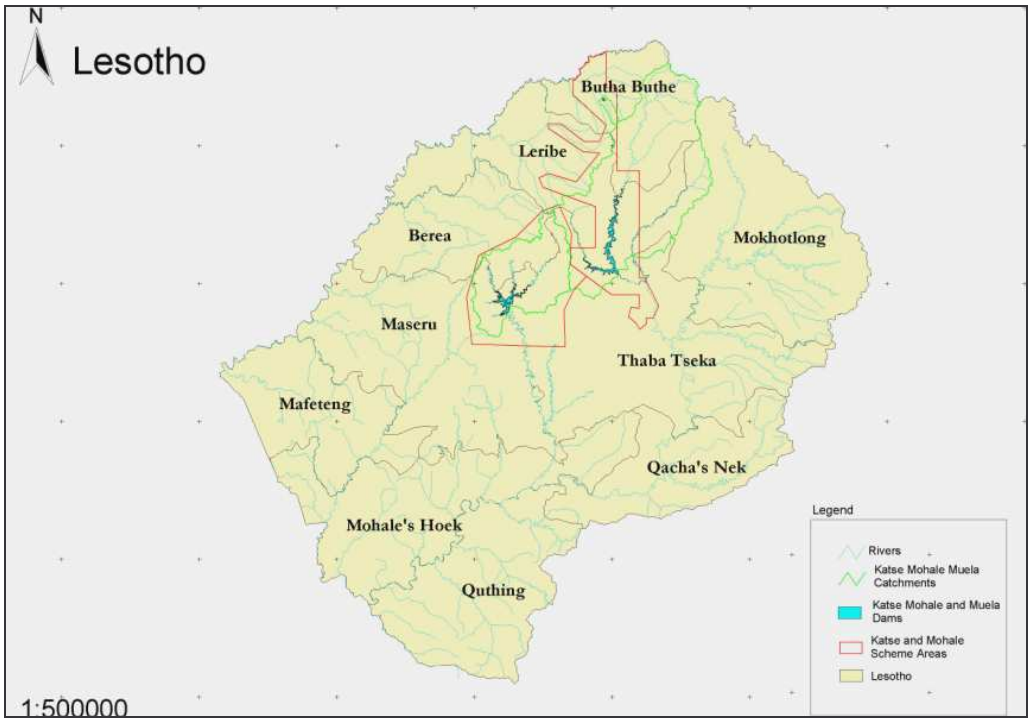

Figure 3.1: Map of Lesotho showing the current Lesotho Highlands Water Project dams. (Map from LHWP).

The region is susceptible to reservoir induced seismicity (RIS) as a result of the dams. A micro-seismic network comprising 11 digital short period sensors is set up to monitor reservoir induced seismicity around the dams. Since the country has no other seismic stations, this network also serves as a national network.

3.1 Network description

Due to recorded case studies of reservoir-induced seismicity (RIS) throughout the world, the LHWP also has to have RIS monitored. The project has two micro-seismic networks adding up to a total of 11 stations, situated at strategic locations around both reservoirs, namely Katse and Mohale Telemetered Seismograph Networks. On average, the stations are about 20 km apart in each network.

Table 3. 1: List of LHWP seismic stations and their locations

LHWP SEISMIC NETWORKS	STATION NUMBER	STATION	CODE	COORDINATES LATITUDE	COORDINATES LONGITUDE	ALTITUDE (MASL)
Katse Dam	1	Katse Dam Office	KTS1	-29.345	28.507	2170
	2	Soai	SOIK	-29.367	28.603	2080
	3	Suaone	SUAK	-29.307	28.395	2300
	4	Mapeleng	MAPK	-29.292	28.497	2160
	5	Mamohau	MHUK	-29.148	28.493	2155
Mohale Dam	6	Mohale Dam office	MOH1	-29.278	28.064	2150
	7	Moholobela	MHLM	-29.304	28.037	2275
	8	Matebeleng	MTBM	-29.245	28.058	2050
	9	VCL Tower	VCLM	-29.281	28.006	2400
	10	Koporale	KPRM	-29.150	28.070	2250
	11	Rapokolana	RPKM	-29.222	28.020	2200

Table 3.1 and figure 3.2 show the LHWP seismic stations and their locations. The stations are labelled by numbers according to the order they appear in the table since they are so densely placed in the figure. MTSN is the Mohale telemetered Seismograph Network and KTSN refers to the Katse Telemetered Seismograph Network

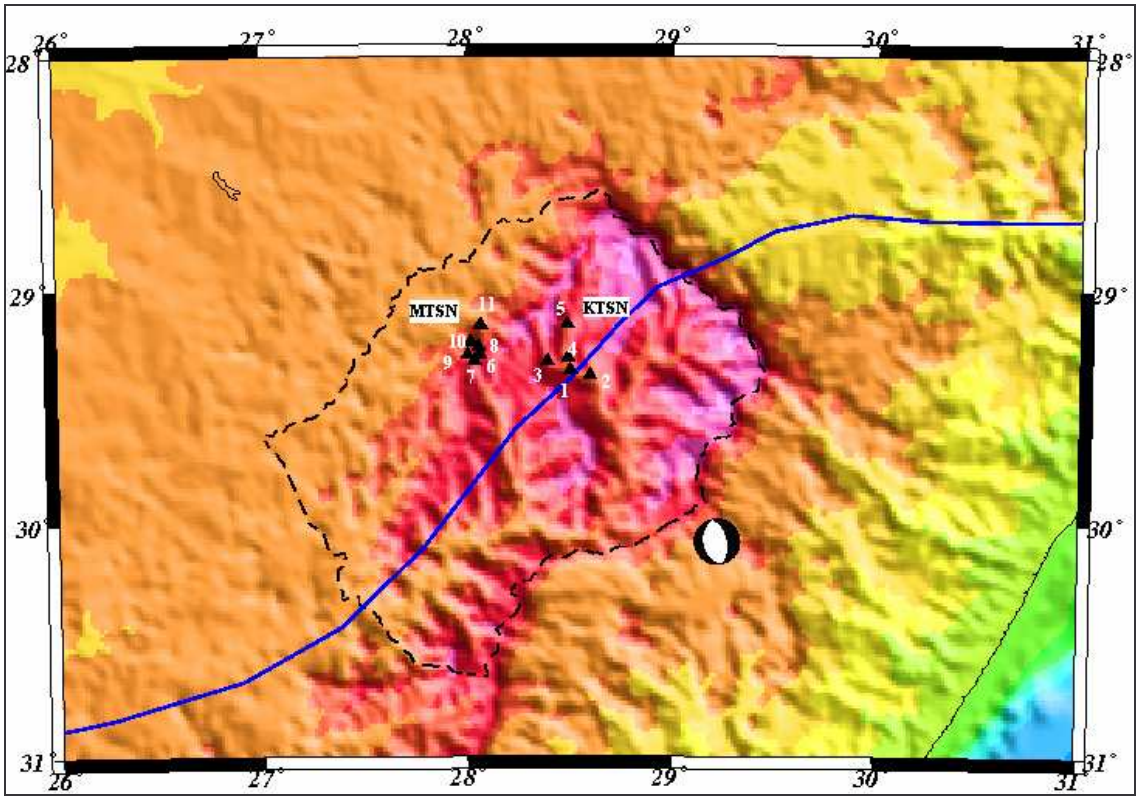

Figure 3. 2: Map of Lesotho showing the location of the seismic stations.

All stations are equipped with three-component, short-period Mark, L4-3C, 1Hz seismometers except for station MAPK that uses an SM6, 4.5Hz geophone. Accurate timing between stations is provided by external GPS units mounted at all stations. Katse dam office and Mohale dam office stations are central sites intercepting data from the remote sites through radio telemetry. These sensors are connected to 24 bit digitizers encased in units termed Multi-Seismometer (MS) event recorders and at the central stations the data is multiplexed and transferred to a computer, known as a Desktop Run-Time System (DRTS). A schematic diagram of a typical station is shown in figure 3.1.

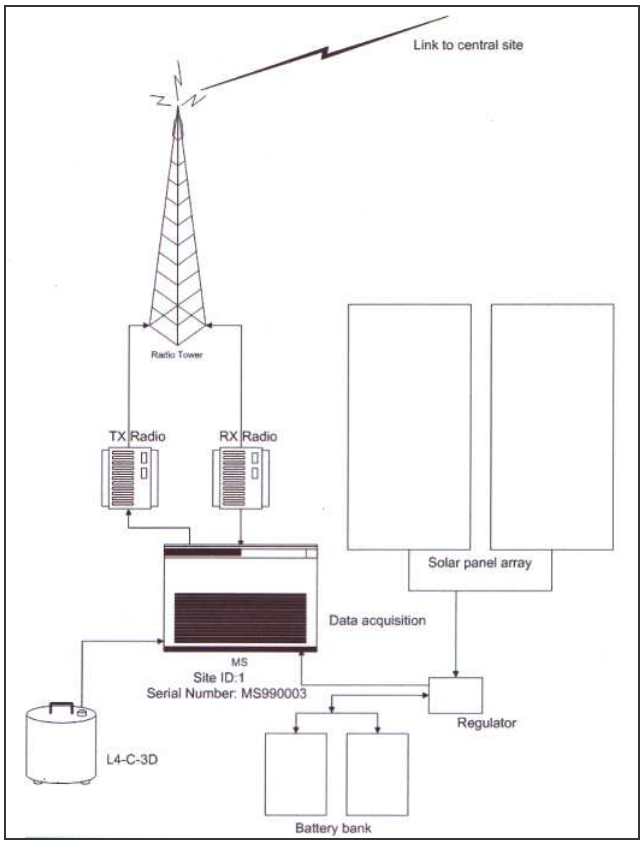

Figure 3.3: A schematic representation of the components of a typical station (Hattingh and Pretorius, 2004)

3.1.1 Katse Network

Katse network began to operate in 1991 originally as an analogue system of three stations then later expanded to five telemetered digital stations around the reservoir area in 1998 (Brandt, 2000). It is made up of one central and four remote stations, which are located to the north – Mamohau (MHUK) and Mapeleng (MAPK), west – Ha Suoane (SUAK) and southeast – Ha Soai (SOIK) of the reservoir. Figures 3.4 and 3.5 show the schematic representation of the KTSN telemetry and a rough sketch of the station distribution all around the reservoir.

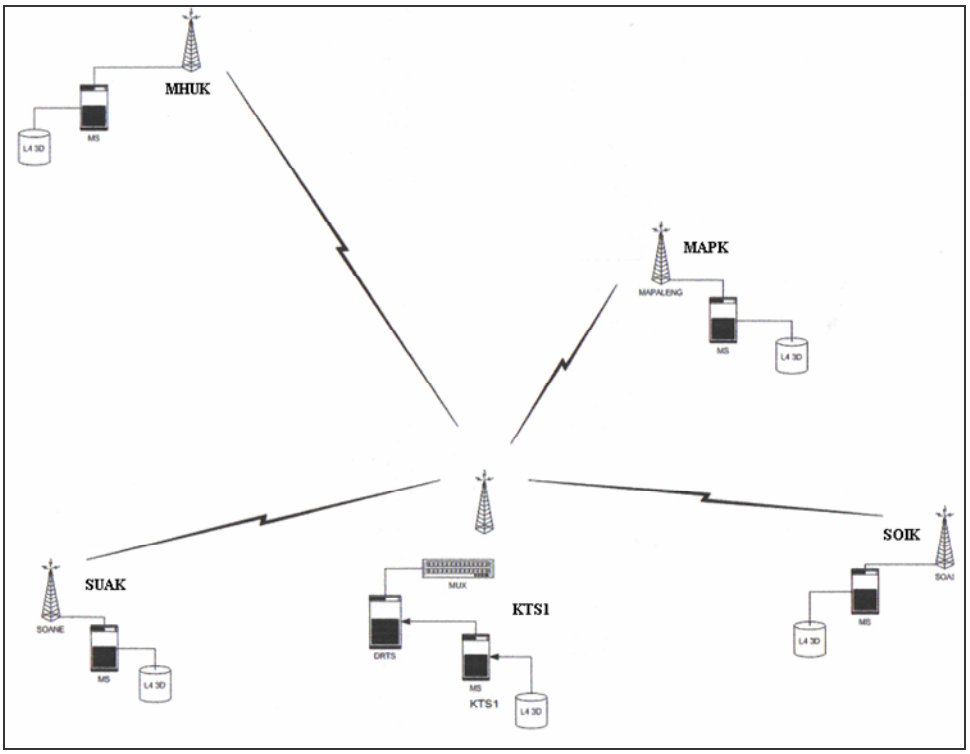

Figure 3.4: A schematic representation of the KTSN telemetry (Hattingh et al., 2004)

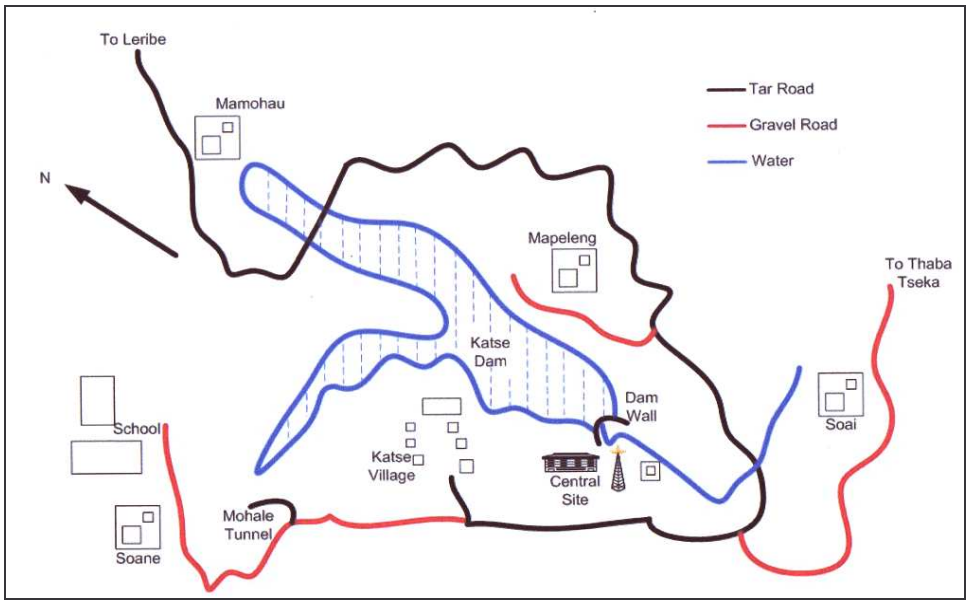

Figure 3.5 A sketch of the KTSN stations in relation to the dam (Hattingh et al., 2004).

3.1.2 Mohale Network

The first station for the Mohale micro-seismic network (i.e. MTSN) was installed in 2001, however, it was only in July 2002 that all stations were in place and fully operational. The central station, with data processing unit, is at the office complex near the dam and five remote stations are located to the northern – Matebeleng (MTBM), northeastern – Koporale (KPRM), northwestern – Rapokolana (RPKM) and VCL Tower (VCLM), southern – Central (MOH1) and southwestern – Moholobela (MHLM) sides of the reservoir. See figure 3.6.

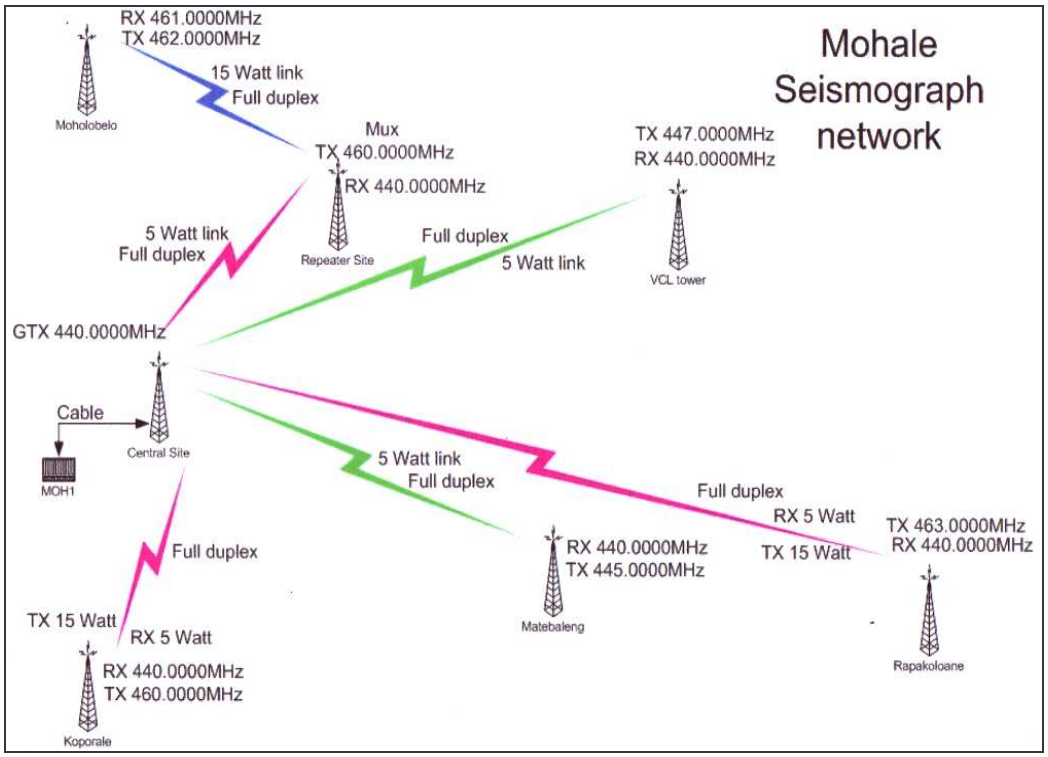

Figure 3.6: A schematic representation of the MTSN telemetry (Hattingh and Pretorius, 2004)

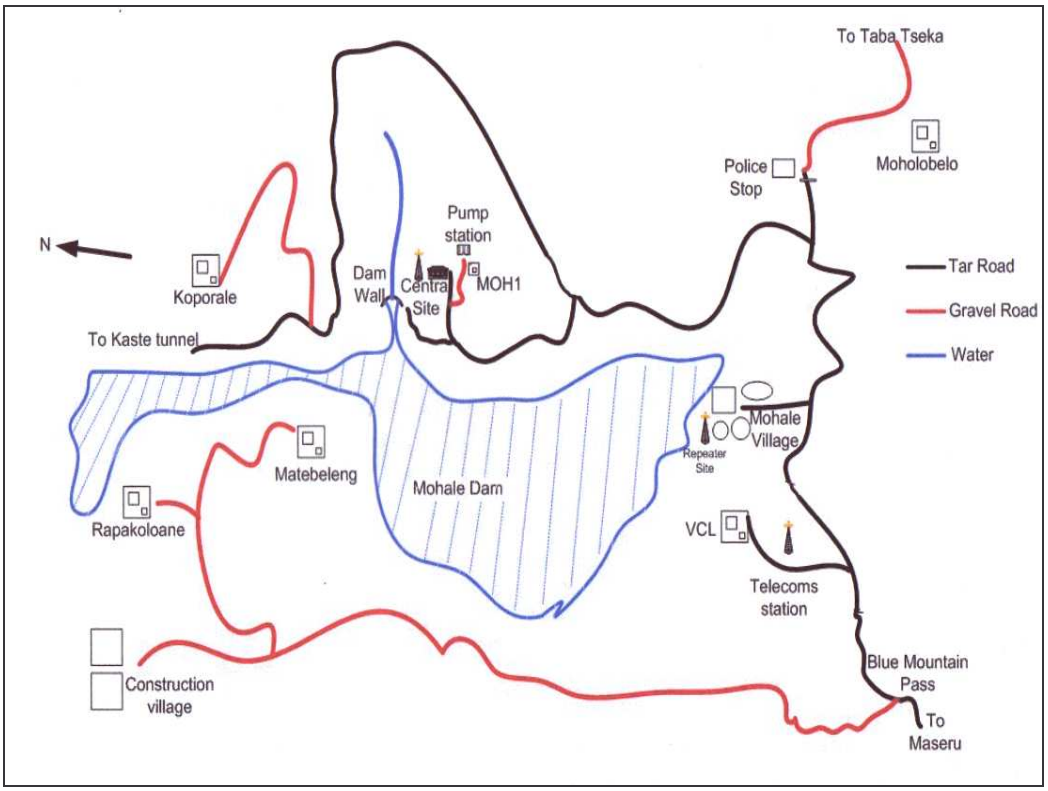

Figure 3.7: A sketch of the MTSN stations in relation to the dam (Hattingh and Pretorius, 2004).

3.1.3. Station Construction

All remote stations comprise an equipment house and a vault (both made of concrete) as well as a guard house. However, two stations of the KTSN are housed in a metal container. In the equipment house, the stations' electronics (i.e. recorders, batteries, voltage regulators and radios) are kept. An external GPS, for synchronized timing and solar panels, for powering the system are mounted on top of the equipment house. The seismometer is housed in approximately 1.5 m deep vault on the side of the equipment house. An antenna mast is also erected on the side to enable communication between the remote and central stations. All stations are fenced with mesh wire. See figure 3.8.

Figure 3.8: A typical LHWP seismic station.

3.1.4. Response Parameters

In order to have the relation between true ground motion and the signals appearing on the computer, two vital factors are required.

i) The true parameters for each unit of a sensor and recorder,

ii) The system's response function, which is defined as:

$$T(f) = \frac{Z(f)}{U(f)} \qquad (1)$$

where f is frequency; Z is the recorded signal and U is the true ground signal (Havskov and Alguacil, 2004). Once the response function is known then it is evident from equation (1) that the true ground motion can be calculated.

A seismic recorder consists of several elements and in order to get the complete response, then the response function of the different elements - which include, seismometer response, amplifier response, filter response and analogue-to-digital converter (ADC) response – evaluated at discrete frequencies, are multiplied together. Tables 3.2 and 3.3

show response parameters for the LHWP network stations, while figures 3.9 and 3.10 are their response curves.

Table 3.2: Response file for all stations except MAPK.

Natural Period	1s
Damping Constant	0.7
Loaded Generator Constant	178
Amplifier Gain	0
Recording Media Gain	1.68×10^{6}
Gain at 1Hz	1.34×10^{9}

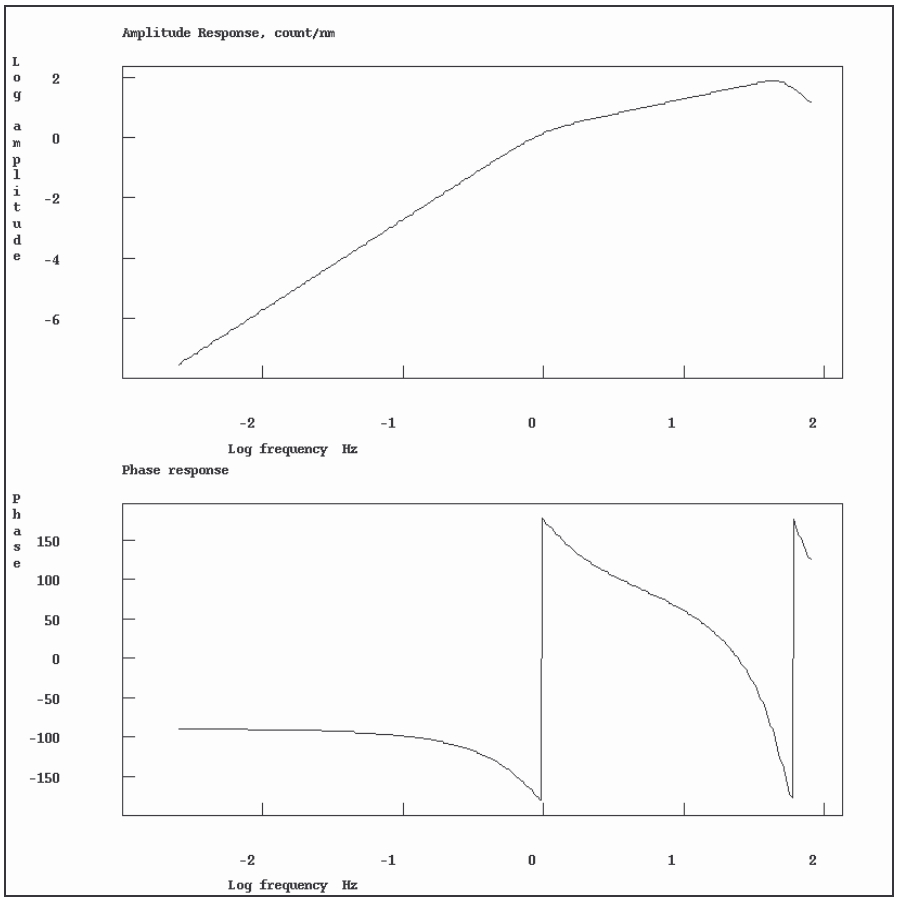

Figure 3.9: Response graph for all stations except MAPK.

Table 3.3: Response file for station MAPK

Natural Period	0.22
Damping Constant	0.72
Loaded Generator Constant	28
Amplifier Gain	0
Recording Media Gain	3.36×10^{6}
Gain at 1Hz	2.86×10^{7}

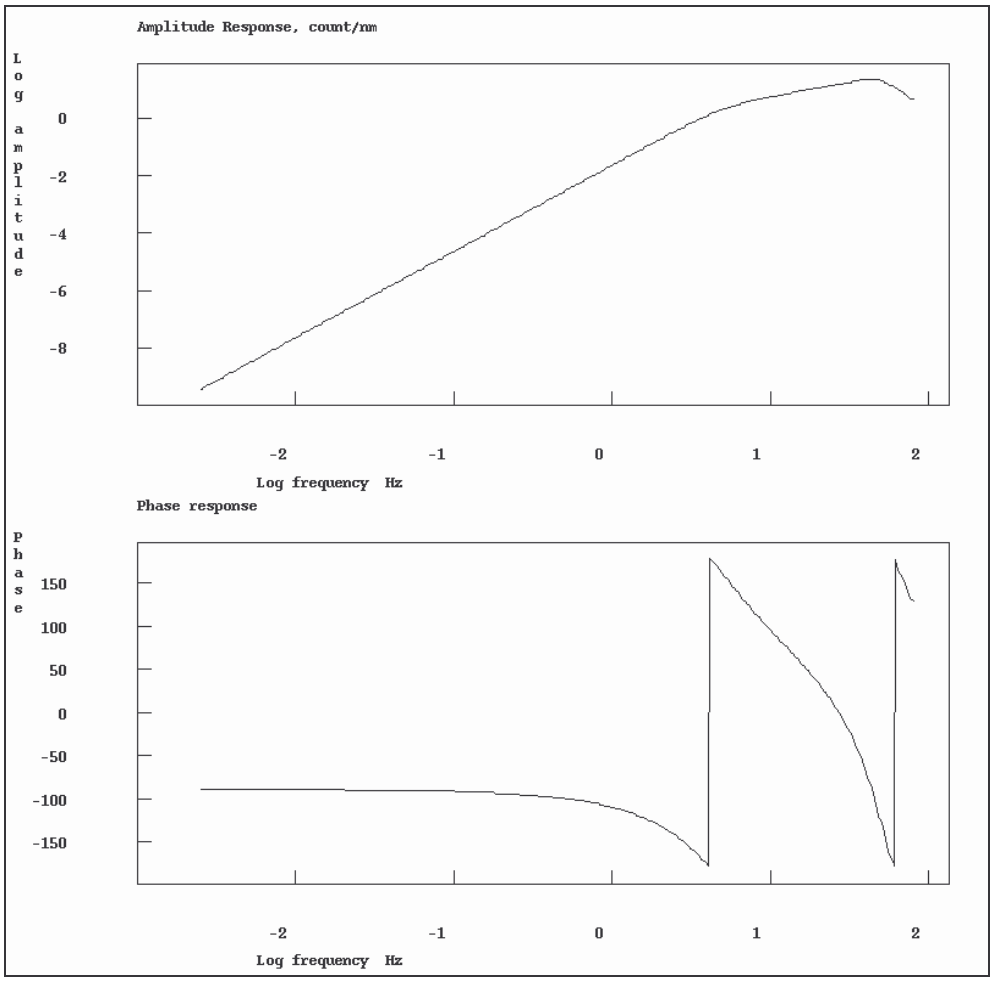

Figure 3.10: Response graph for MAPK.

3.2 Noise Measurements

Two GBV – 316 instruments were taken to Lesotho over the period June to August 2006, for 2 main reasons.

1) To monitor the general seismicity of the country at different sites within the country (i.e. not at the existing seismic stations) – instrument 1.

2) To test the noise level at the existing seismic stations – instrument 2.

3.2.1 Instrument Description

The GBV – 316 is a 16-bit digital seismic data acquisition system with tri-axial in-built 4.5Hz geophones in portable weather-resistant aluminium cast housing. A standard 12V lead-acid battery powers the instrument although it is equipped with an internal battery that can be used for up to 24 hours. Figures 3.11 is a picture of the GBV – 316 while figure 3.12 is its response curve and table 3.4 gives the instrument's response parameters.

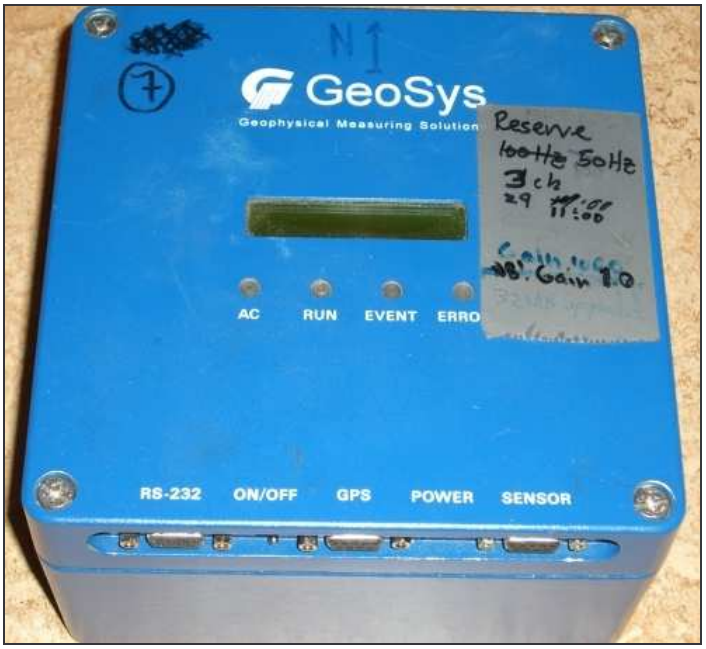

Figure 3.11: A picture of the GBV-316 unit.

Table 3.4: Response file for station GBV.

Natural Period	0.22s
Damping Constant	0.72
Loaded Generator Constant	28
Amplifier Gain	0
Recording Media Gain	1.28×10^{7}
Gain at 1Hz	1.09×10^{8}

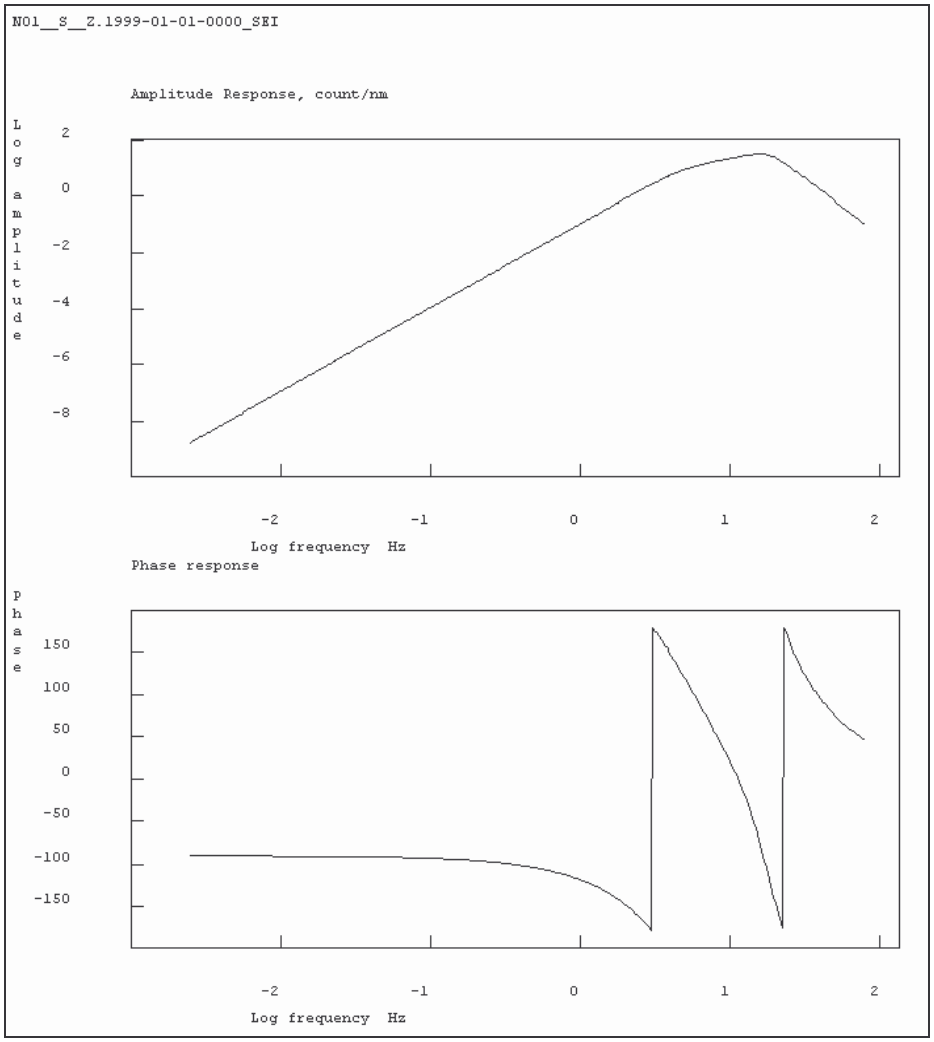

Figure 3.12 GBV response file.

3.2.2. GBV-316 Operation

In order to operate the instrument (GBV-316), it has to be connected to a personal computer with an RS232 communications port. This connection enables one to Configure the GBV and in this way, the parameters can be set up for recording as a stand-alone unit (Aranda, 2000). The accurate time stamping of the data is achieved by connection of an external GPS to the GBV.

There are two ways in which the instrument can be set up to record events, which are namely, the trigger mode and continuous recording mode. A trigger is an algorithm that checks the signal for variations that could indicate an event(Havskov and Alguacil, 2004). The triggering parameters and are set up by the menu driven set-up program "AllView"(Asl, 2000). By trigger method, the instrument will make a recording only when there is an event, while continuous recording simply means that the instrument keeps recording for as long as it is operational.

3.2.3. GBV-316 Data Collection

Instrument 1

Instrument number 1 was used to investigate recordings at 3 different locations within the country of Lesotho; namely: a) 'Muela (representing the Northern part)

b) Mohale's Hoek (for the Southern part)

c) Semonkong (central eastern part)

In figure 3.13, the red dots indicate the location of the 3 temporary sites. The black colour filling parts of the rivers in the central part of the country represent the complete part of the LHWP.

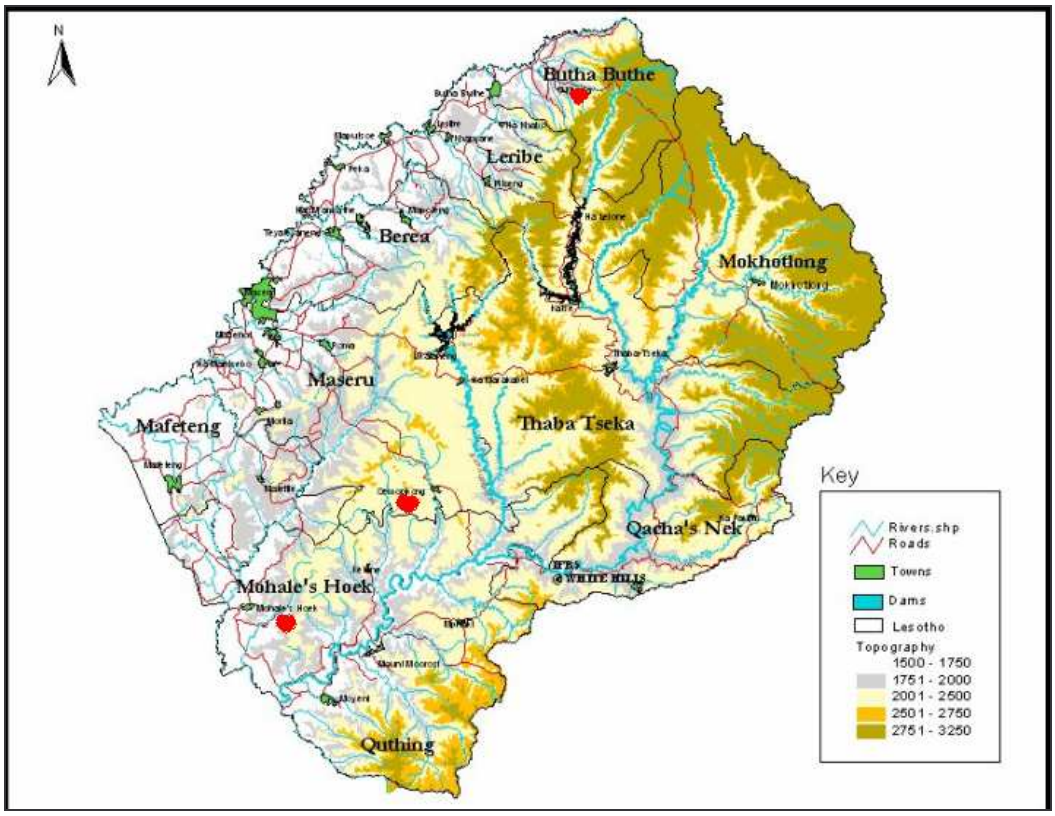

Figure 3.13: *A topographic map of Lesotho showing the major towns and the LHWP region. Katse and Mohale dams are in black colour. The red dots indicate the location of the temporary stations.(Map fromLHWP).*

3.2.3.1. Site 1 – 'Muela Hydro-Power,Surge shaft

The first site (i.e. 'Muela) was established on June 21, 2006 near the 'Muela Hydro-Power surge shaft. See table 3.5 for location details. The 'Muela Hydro-Power plant is part of the Lesotho Highlands Water Project and this site represented the northern part of the country and was chosen in view of the fact that there is a 24 hour security service. The surge shaft is located at about 200m from the hydro–power plant. The purpose of the shaft is to absorb the energy of the water and allow it to oscillate during emergency closures of the power plant (i.e. such that it does not flow back to the main storage). Due to its location, this site's results were expected to contain a bad signal to noise ratio but as can be seen in figure 3.14, the station has a good ratio, since the curve falls within the Peterson high and low noise model.

Table 3.5 Location & installation time for site 1 – 'Muela.

Latitude	28^0 46.976S
Longitude	28^0 27.105E
Altitude	2108
Time	11:47

This instrument was set up and left recording continuously, overnight at intervals of 20minutes (i.e. 1200s). Although 72 events were expected, only 44 were recorded. On the second day, the instrument was set up to record on "trigger mode"; three jumps were made to verify that this would work and the GBV recorded them. The instrument was left overnight again, to record in "trigger mode". This mode ensures that the instrument will make a record only when an event occurs as opposed to the "continuous mode", which records continuously.

The trigger parameters were set as can be seen in table 3.6 and these were used for all the sites:

Table 3.6: Trigger parameters used for GBV instruments set up in Lesotho.

STA	4 s
LTA	150 s
STA/LTA	14 dB
Pre-event memory	10 s
Post event memory	10 s
Turn-on-delay	10 s

On June 22, 2006 the GBV was checked for the previous night's (i.e. June 21) records. Except for seven traces which were noise signals, no events were recorded.

The instrument was left at site 1 for 15 days (i.e. until July 07, 2006) and 75 records were made to the GBV. Out of these 75 only 3 were real seismic (regional) events located in South Africa and the rest were seismic noise signals. Figure 3.15 shows one of the events recorded by this station.

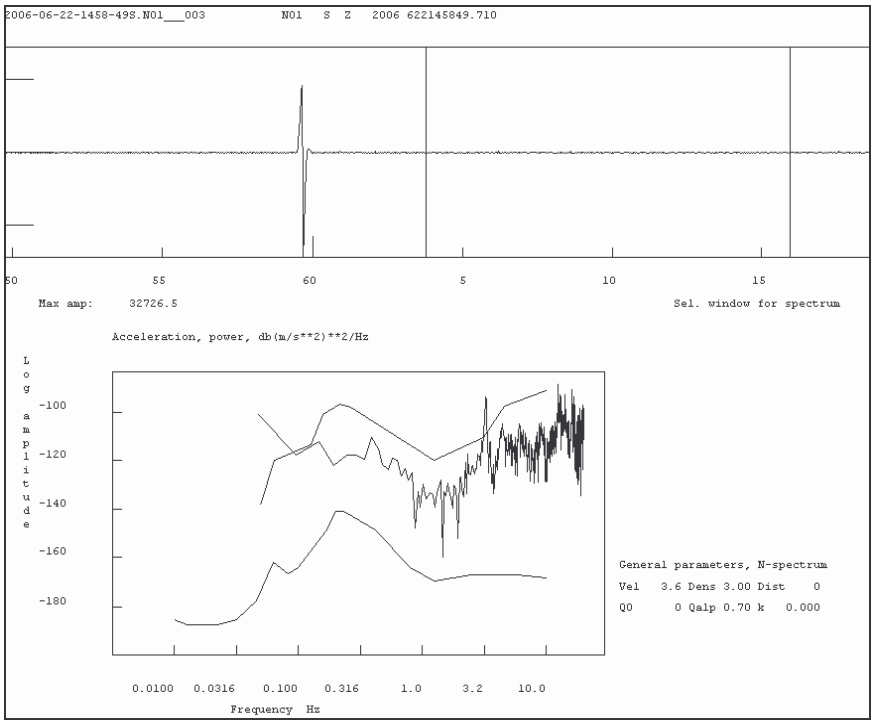

Figure 3.14: Typical seismic noise from site 1 (‘Muela), as well as its noise spectrum.

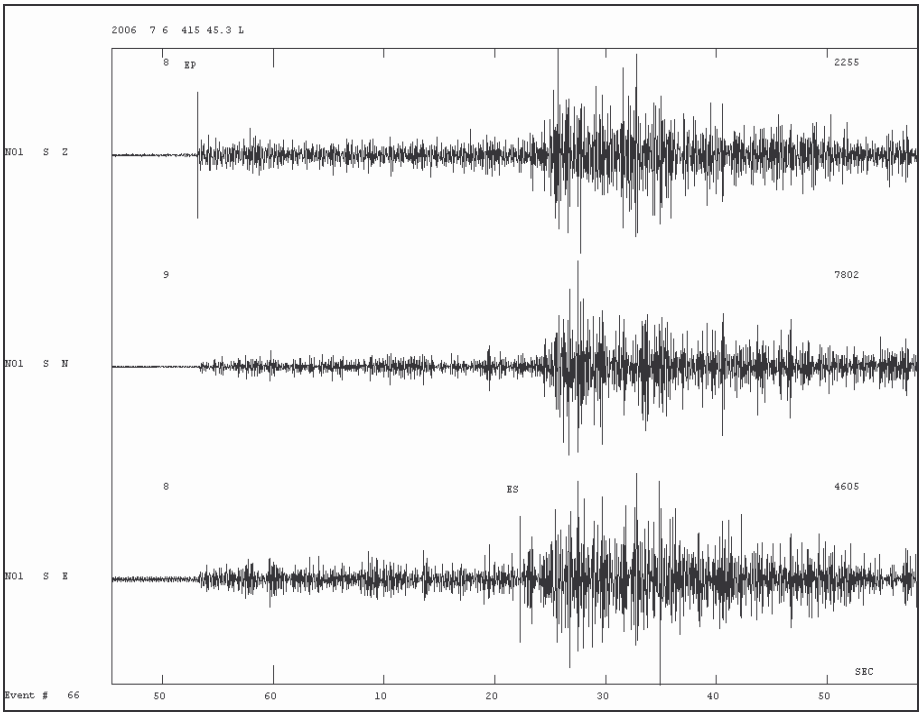

Figure 3.15: Plot of an event recorded by the GBV at site 1.

3.2.3.2. Site 2 – Mohale's Hoek, St. Stephen's High School

This site was established on July 08, 2006 and was set up to record for 14 days (i.e. until July 22, 2006). This site is located at the St. Stephen's High School teachers' residence and represented the southern part of Lesotho. There is a main road about 100 m away from the station which is the closest source of noise. In this period, 290 seismic signals were recorded, one of which was also a regional event located in South Africa. Location details for this site are given in table 3.7. Figure 3.16 shows a typical seismic noise signal and spectrum recorded at this site and 3.17 shows an event that was located in south Africa.

Table 3.7: Location & installation time for site 2 – Mohale's Hoek

Latitude	30^0 08.982S
Longitude	27^0 28.182E
Altitude	1568
Time	11:30:46

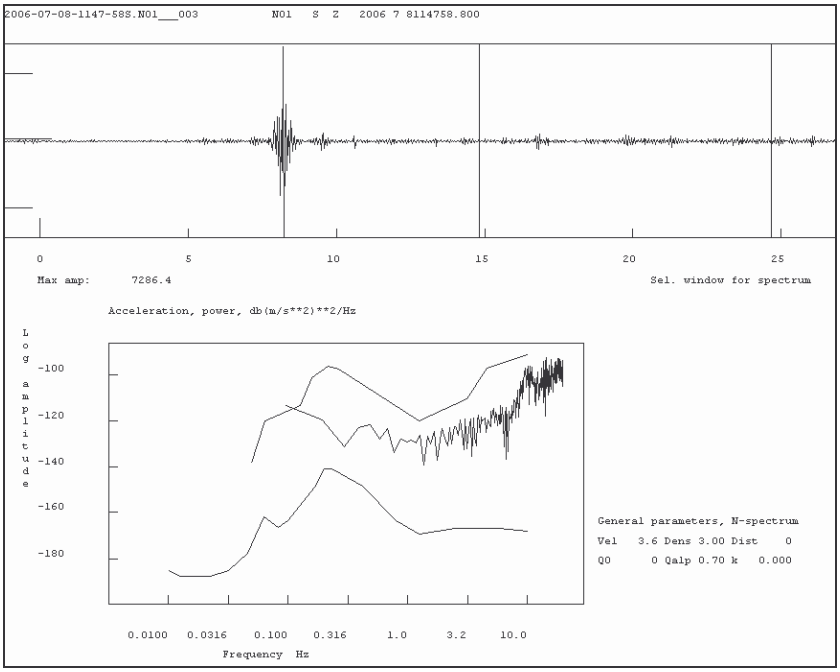

Figure 3.16: Noise signal and its spectrum from site two (Mohale's Hoek).

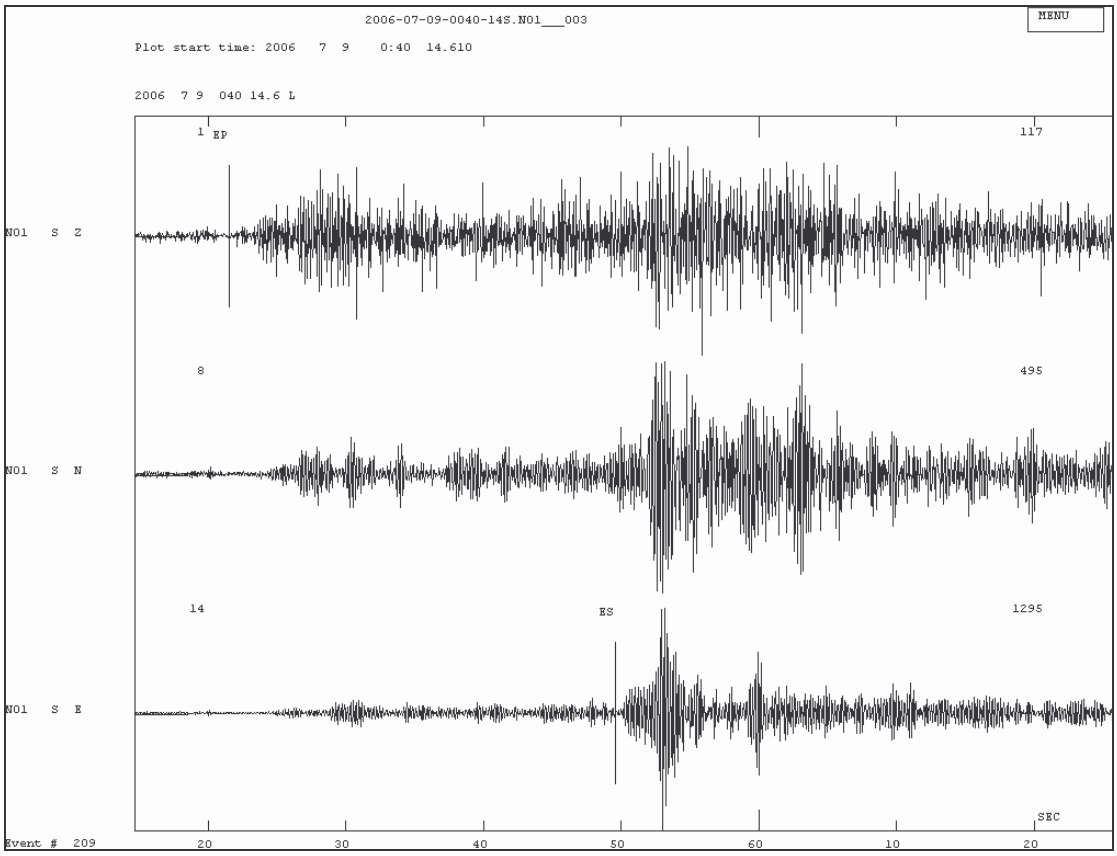

Figure 3.17: Earthquake signal recorded at site 2.

3.2.3.3. Site 3 – Semonkong, TeleCom Lesotho Tower (TCL)

Semonkong is one of Lesotho's major tourist attractions due to the Maletsunyane falls – the highest single-drop waterfall, at 197m, in the southern hemisphere. The site was situated about 15km from the fall at one of the country's telecommunication (TCL) tower sites. This site was chosen to represent the central part of the country.

Site 3 was established on July 23, 2006 and set up to operate for 20 days (i.e. until August 12, 2006). Unfortunately, during these three weeks (from July 1st) Lesotho had the heaviest of snowfalls and as can be seen in table 3.9, the station location was at the highest altitudes of all three stations. Even without snow, the site was very windy and cold. On August 12, 2006 the GBV was found malfunctioning and the battery was drained well below operational limits. From the records, it appears that the instrument

was functional for the first 6 hours after deployment and only 5 records were made, all of which were seismic noise.

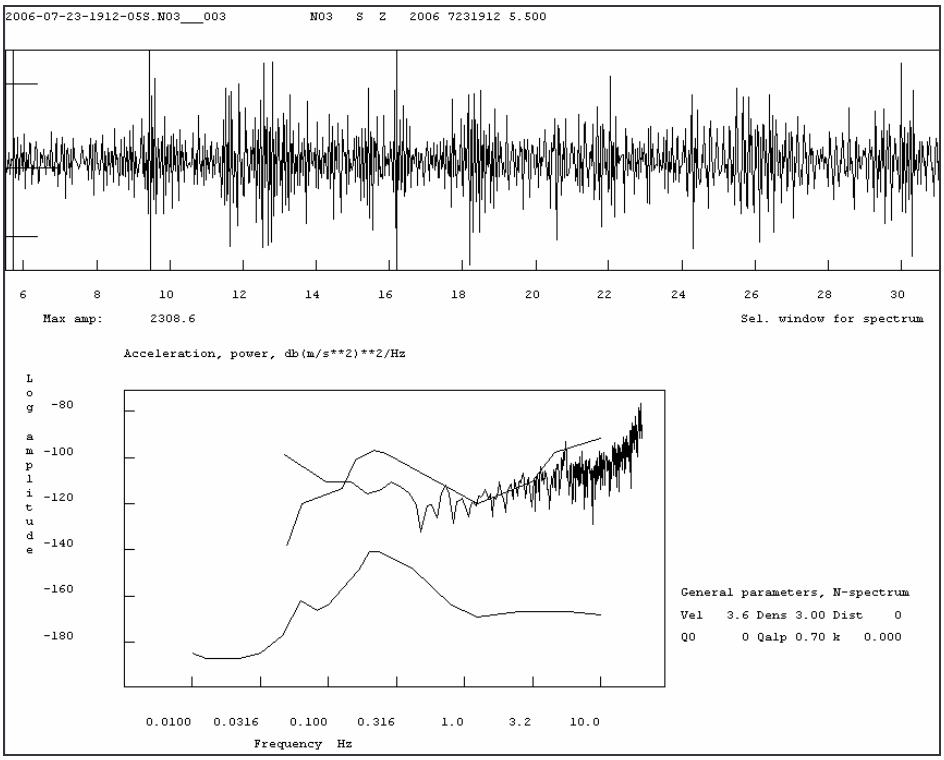

Figure 3.18: Typical noise signal and its spectrum at site 3.

Figure 3.18 shows a typical seismic noise and noise spectrum from this station and as expected the signal to noise ratio was not very good.

Table 3. 8: Location & installation time for site 3 - Semonkong

Latitude	29^0 50.381S
Longitude	28^0 06.331E
Altitude	2707
Time	12:45:28

3.2.4. Instrument 2

The second GBV –316 was to be installed at the already existing Lesotho Highlands Water Project's (LHWP) seismic stations. However, it was not possible to place the GBV exactly alongside the permanent stations. Due to the lack of manpower, the vaults in which the permanent sensors are housed could not be accessed as they are covered with heavy concrete blocks; instead the GBV's were placed as close as possible to the vaults.

Between August 10 and 16, 2006 instrument 2 was setup at the different permanent stations to record for between 30minutes to several hours. Table 3.10 shows the location details of the temporary stations at the permanent stations.

Table 3.9: Location details of instrument 2 at the different permanent stations.

	SOIK	VCLM	MHLM	MOH1	RPKM	MTBM
Latitude	29^0 22.148S	29^0 28.011S	29^0 20.041S	29^0 18.408S	29^0 13.504S	29^0 15.039S
Longitude	28^0 35.761E	28^0 00.699E	28^0 04.132E	28^0 04.35.2E	28^0 02.588E	28^0 02.490E
Altitude	2148	2560	2388	2302	2364	2210
Date	10/08/07	15/08/07	15/08/07	15/08/07	16/08/07	16/08/07
Time	11:58:18	07:56:39	09:12:22	12:26:39	10:18:23	14:03:47

The GBV results are in accordance with the permanent stations and the local network stations seem to have noise levels that fall within the Peterson curves. Plots of the noise spectra comparisons are in Appendix B. Figure 3.19 shows an example of a noise power density spectrum showing the high noise model and low noise model.

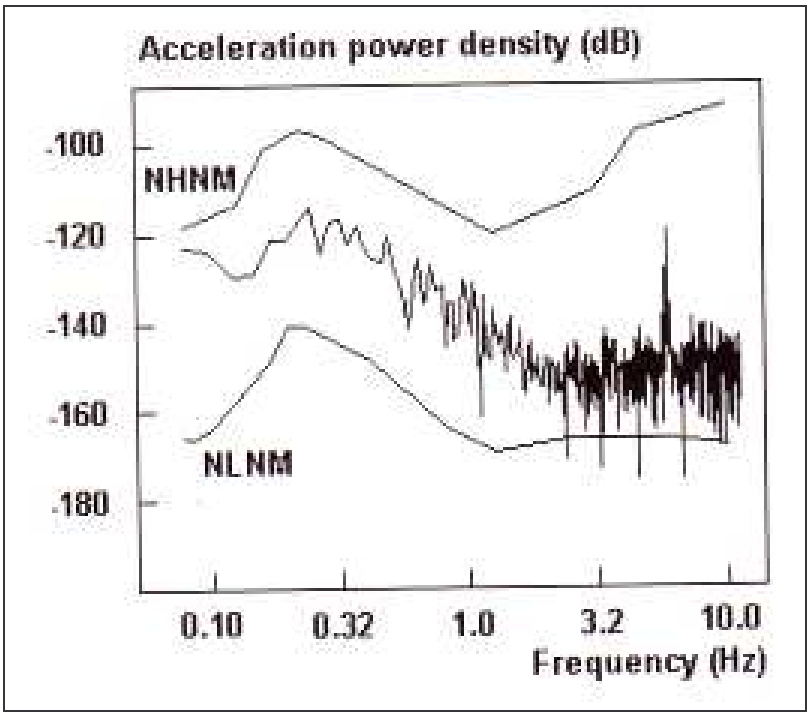

Figure 3.19 *Example of a noise power density spectrum of a raw signal, showing the Peterson noise model limits indicated by NHNM and NLNM (Havskov and Alguacil, 2004).*

3.3 Network Operation and Operational Statistics

3.3.1 Network Operation

The two networks are data linked by telephone dial-up through modems, which enables remote monitoring of KTSN from Mohale (MTSN). The remote stations are powered by solar energy with the use of solar panels, regulators and batteries, while the central stations are electric powered. The recorders with built-in digitizers (i.e. MS event recorders) are designed in such a way that data is accumulated at the remote stations through triggering algorithm. After integrity check the data is then transmitted to the central station through radio telemetry where it is stored on a computer (also known as a Desktop Runtime System –DRTS). Once transmitted, the data is automatically deleted from the recorder, to free memory space so new data can be accumulated. The timing at all the stations is provided by satellite through Global Positining Systems (GPS).

Functional tests ("state-of-health-checks") are run daily at the Mohale central station, in order to monitor the status of the remote stations. In case the data link is malfunctioning, then the tests/checks for the KTSN are run at its central station.

Data is retrieved and saved onto CD's then analysed with the use of SEISAN software on a dedicated analysis computer at Mohale (i.e. MTSN).

3.3.2 Operational Statistics

During their existence, the seismic networks have experienced numerous downtimes, which were, for a long time, attributed to lightening. It was recently discovered that even in times when there are no rains (which usually go with lightening), the networks are still subjected to failure. A number of speculations, which include: telemetry problems have been deliberated on this matter.

The operational statistics history of the LHWP seismic stations can be found in Appendix A.

3.4 Data Reprocessing

The archived LHWP data used in this study spans from February 2002 to December 2006. First, a database was created, and then the data was copied month by month, for the respective years, from the backup CD's to the working directory. Since data from the earlier years was backed up using an older version of the SEISAN software, a conversion from ASCII to binary had to be done.

Raw seismic signals were evaluated using SEISAN (Havskov and Ottemöller, 2005)in such a way that events were selected and kept if only they were recorded by two stations or more. The selection was done in this manner owing to the fact that there were lots of files to sieve through and also with the thought that a significant event would at least be recorded by more than one station. With reference to table 3.2, this criterion, however,

meant that those events recorded by one station, when other stations could have been malfunctioning, would then be missed out.

The individual events were merged together if they occurred within two minutes (i.e. 120 s) of each other. Once the extraction was complete, signal processing followed and events were then registered in the database with their respective identities. Since it was rare that records would be registered by more than two stations, the location of events was done using the single-station location procedure. In the end, there were 711 events registered, of which 139 were local, 522 regional and 50 teleseismic. Both regional and teleseismic events were verified with the International Seismological Center (ISC) and Prelimenary Determination of Epicenters (PDE).

Due to the short window length of the signals, not many of the events exhibited their full coda lengths and as a result the local magnitude scale –as defined by Richter- was the most used. There are however, few events with coda magnitudes.

Since seismic analysis for LHWP was carried out by the South African Council for Geoscience,in the beginning, the velocity model used for locating the events is based on their model (i.e. South African model) and can be seen in table 3.11.

Table 3.10: Velocity model used for locating earthquakes in this study (V_P/V_S=1.74).

P-wave velocity (km/s)	Depth (km)
6.18	0.0 – 35.5
8.27	>35.5

3.5 Data Description

As mentioned in section 3.4, the re-analyzed LHWP data, for the period February 2002 to December 2006, consists of 711 events comprising 139 local events of which 66 are associated with blasting incidences during the construction of the Mohale Dam and feeder roads. This part of the data is available in waveform files as well. Figure 3.20 shows earthquake distribution in the region of Lesotho for the period 2002 to 2006.

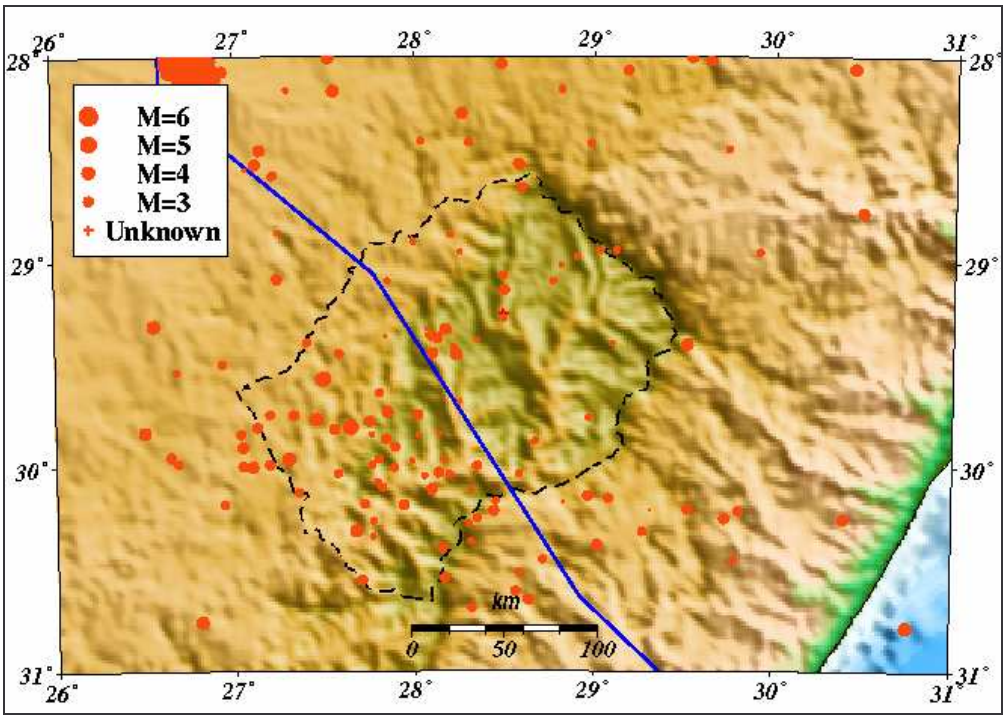

Figure 3.20: *Map showing earthquake distribution in the region of Lesotho for the period 2002 to 2006. This plot excludes all blasting events (i.e. known explosions). The total number of events in the figure is 396. The blue line represents the tentative plate boundary as suggested by (Bird, 2003).*

Parametric data from previous thesis work (Brandt, 2000) was incorporated to this data since it is also from the LHWP. More parametric data from ISC and the South African Council for Geoscience (CGS), which includes historical data, is added to the database. All in all the data spans from 1620 to the end of 2006. With all the catalogues merged together, the total number of earthquakes is 2586. There are 363 local, 2173 regional and 50 teleseimic events. Two major events of magnitude $M_L \geq 5.0$ have occurred within the borders of Lesotho. One event of magnitude $M_L = 5.0$ occurred in 1966 in the North-Eastern part of the country and another of magnitude M_L 5.1 occurred in 1986 in the southern part. Two other events of $M_L = 4.7$ and 4.6 occurred 20 minutes apart on January 27, 2002.

3.5.1. Missing data

As mentioned above, a total of 711 earthquakes was found, 224 of which are within the study region. A comparison of this part of the data was made by checking the ISC records and table 3.12 shows the different statistics.

Table 3.11: A statistical table for comparison of the network detection capability.

Agency	Total number of earthquakes	Number of local earthquakes	Number of Regional earthquakes
ISC	308	-	308
LHWP	224	98	126

From the table above, it is evident that 84 earthquakes are missing and the ISC catalogue has no record of local events. This could result from the fact that ISC's detection threshold is higher than what is recorded in the area; or the loss of data during the networks' downtimes. Alternatively, this difference could be due to the loss of data during analysis. On the other hand, the earthquakes which were recorded by the temporary stations (i.e. GBV-316), were not recorded by the local network stations that were functional during the "Noise measurements" experiment.

Even though the criteria for selecting events was by choosing those earthquakes recorded by two stations or more, few known events that were recorded by one station, were incorporated into the database, however, no earthquakes were found recorded by seven or more stations. See Table 3.13.

Table 3.12: The number of events per number of stations recording them. No events were recorded by more than 7 stations.

Number of stations	**Number of events**
1	62
2	98
3	48
4	12
5	1
6	3

The ISC catalogue has a total of 1044 earthquakes located in the study region, with the first record in the year 1957, which means 333 of these earthquakes are missing for the local network data.

3.5.2. Detection threshold for Lesotho

In order to have a true picture of the general earthquake distribution of Lesotho, data was sourced from two other agencies, the Council for geoscience (CGS) and the International Seismological Center (ISC). These were incorporated to the local data and a catalogue was compiled. This procedure is discussed in detail in section 5.1.2.

Since a significant number of events are missing, the detection threshold was determined in order to identify which magnitude were not recorded. Figure 3.21 shows the detection threshold of the local network. The a- and b-values are 5.29 and 0.98, respectively.

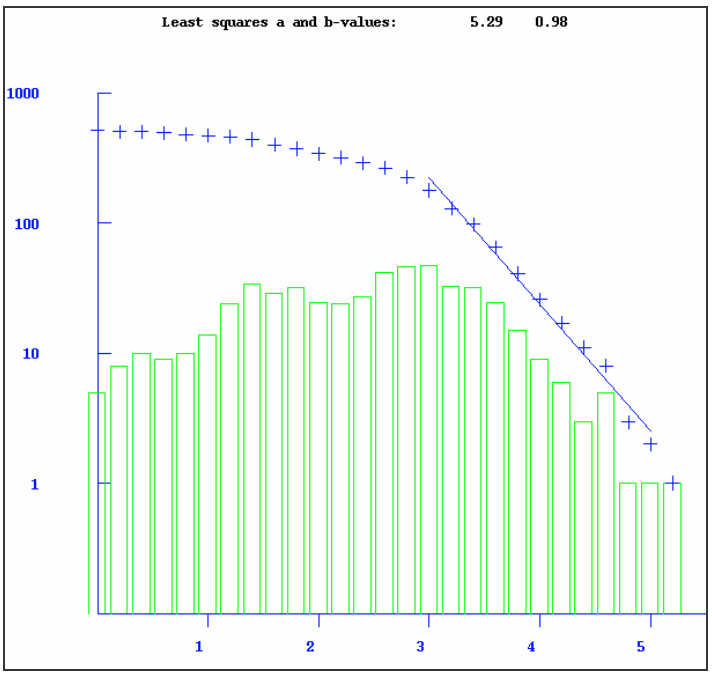

Figure 3.21: b-value plot for the local data. From the plot it is evident that the detection threshold is between M_L 2.8 and 3.0. The data used in this plot is from the local network only. It is clear that the detection threshold is around magnitude 3.0.

4 Analysis of Local Network Data

4.1. Local Seismicity

From chapter 3, it can be seen that there is a significant amount of data missing and this could be attributed to several reasons. These reasons include:

- Stations' downtimes

The stations have functioned intermittently since their installation; moreover it is unclear what the real reason for their malfunctioning is.

- Inadequate detection capability

It is thought that the trigger parameters could have been set to low, thereby resulting in loss of some data that should be recorded.

- Timing problems with some of the stations

During the analysis, three stations were identified with a clock error problem and this is thought to be a possible contribution for some of the missing data.

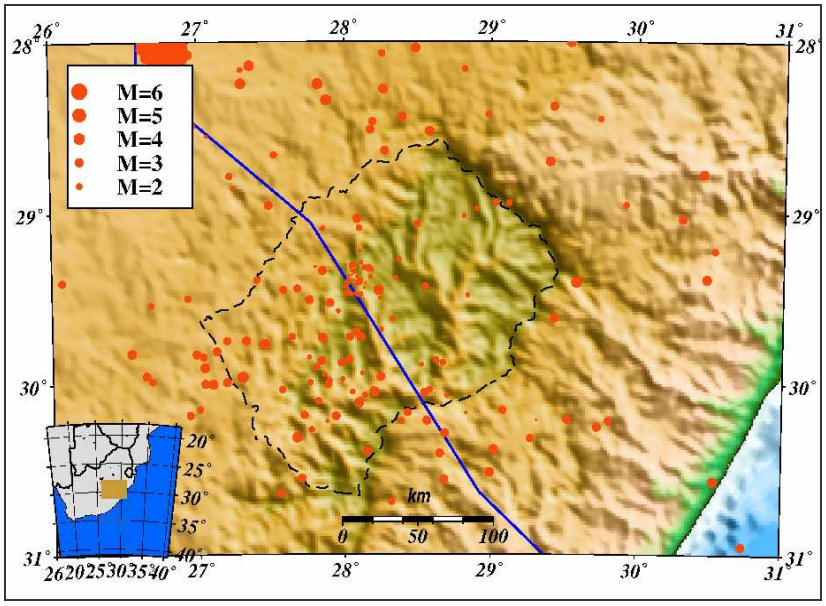

Figure 4.1: Map of seismicity in the study area. The total number of earthquakes is 711.

Despite the above-mentioned problems, it is clear that Lesotho is characterized by a seismically active zone in the southern part. This is in consistency with what has been observed and recorded in existing literature.

4.2. Coda Q and Magnitude Scales

4.2.1. Coda Q

Quality factor Q is an important property that has been used throughout the world to study the attenuation of seismic waves in the lithosphere. Large values of Q indicate low/small attenuation.

Coda waves are a result of a sequence of arrivals of scattered seismic waves due to heterogeneties in the lithosphere (Lay and Wallace, 1995). According to (Aki and Chouet, 1975) the coda wave amplitude is said to decay with time by the following expression:

$$A(f,t) \Rightarrow S(f) * t^{-u} * e^{\frac{\pi * f * t}{Q(f)}} \tag{4}$$

where A is the coda amplitude, at frequency f with S(f) as the earthquake source function. Q(f) is the quality factor at f, u is the geometrical spreading and t is the time from origin.

The Q is determined from coda waves (Aki and Chouet, 1975; Havskov et al., 1989) and is observed to increase with increasing frequency for frequencies between 0.1 and 30Hz (Mitchell, 1981) and tectonic activity. This frequency dependent Q is described as follows:

$$Q = Q_0 f^{\alpha} \tag{5}$$

where, f is the frequency, Q_0 is the value of Q at 1Hz and α is a constant ranging from 0.5 to 1.5 (Singh et al., 1983). Q is also observed to increase with depth (Roecker et al., 1982).

Using data from all the LHWP stations in the database, coda Q is calculated for 96 earthquakes, since not all data has both phases present. Due to the few data that is used, several trials were made to calculate Q using different input parameters and three reasonable values were obtained for the frequency range 1-24 Hz. The values of $Q_0 = 45$ and $\alpha = 1.26$ are used for calculation of moment magnitude (see section 4.2.2). Table 4.1 is a least of the relatively good values obtained and figure 4.2 is an example of the plots.

Table 4.1: Realiable Q and Q_α values calculated.

Window length (s)	Q_0	α
12	45	1.26
10	41	1.20
8	33	1.0

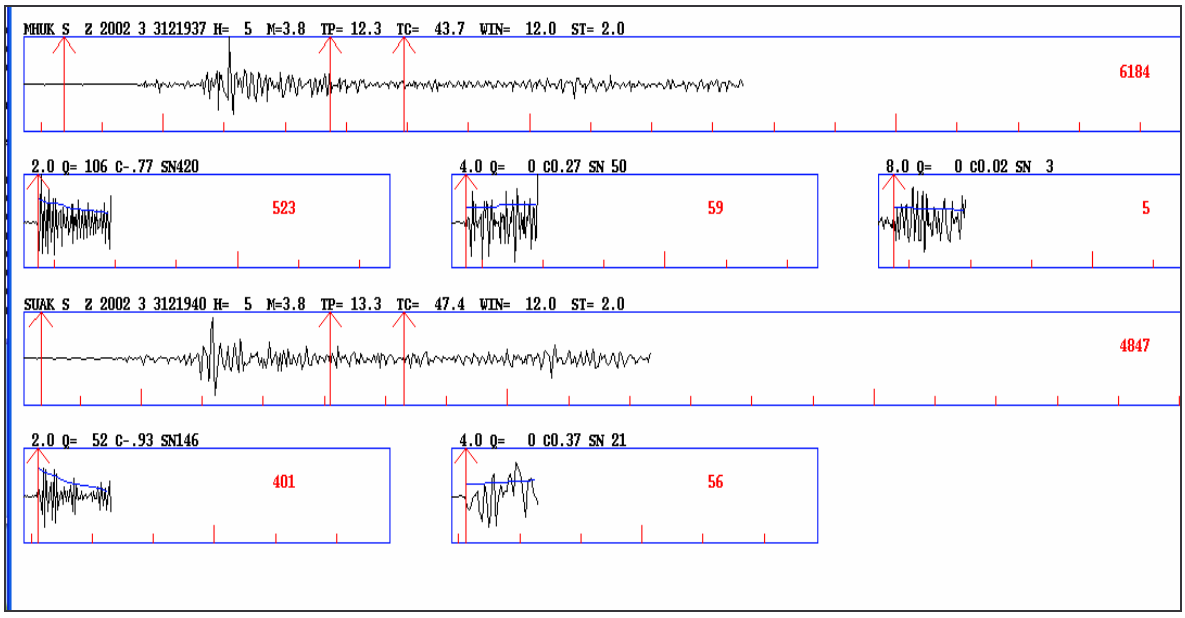

Figure 4.2: Coda Q calculated for 6 events.

4.2.2. Magnitude scales

When compared, the magnitudes calculated locally are in consistency with those from other agencies. It is important to note that most of the earthquakes in the other catalogues used are located using the local Richter magnitude. In table 4.2 a summary of the number of earthquakes with different magnitude types is given.

Table 4.2: Distribution of the different magnitudes in this study's catalogue (including explosions). Some events are reported with more than one magnitude type.

Magnitude type	**Number of earthquakes**	**Total number of earthquakes**
M_L	1048	1265
M_C	133	
M_W	126	
M_b	115	
M_S	6	

As it can be seen in table 4.2, M_L is the most reported magnitude type (about 80%) therefore an attempt to convert the magnitudes proved to be impractical. More about this can be seen in chapter 5.

4.2.3 Moment Magnitude

Once the coda Q was calculated, the values of Q_0 and Q_α were changed in the MULPLT.DEF file, in SEISAN. Moment magnitude was calculated after coda Q had been computed however, this resulted in too few events to make a conversion between any two magnitudes. Figure 4.3 is a map of showing the events reported with moment in the study region.

Comparing to the number of events in table 4.2, it is apparent that the rest of the events with magnitude are out of the region of study. It seems the rest of the events with M_W are outside the study region.

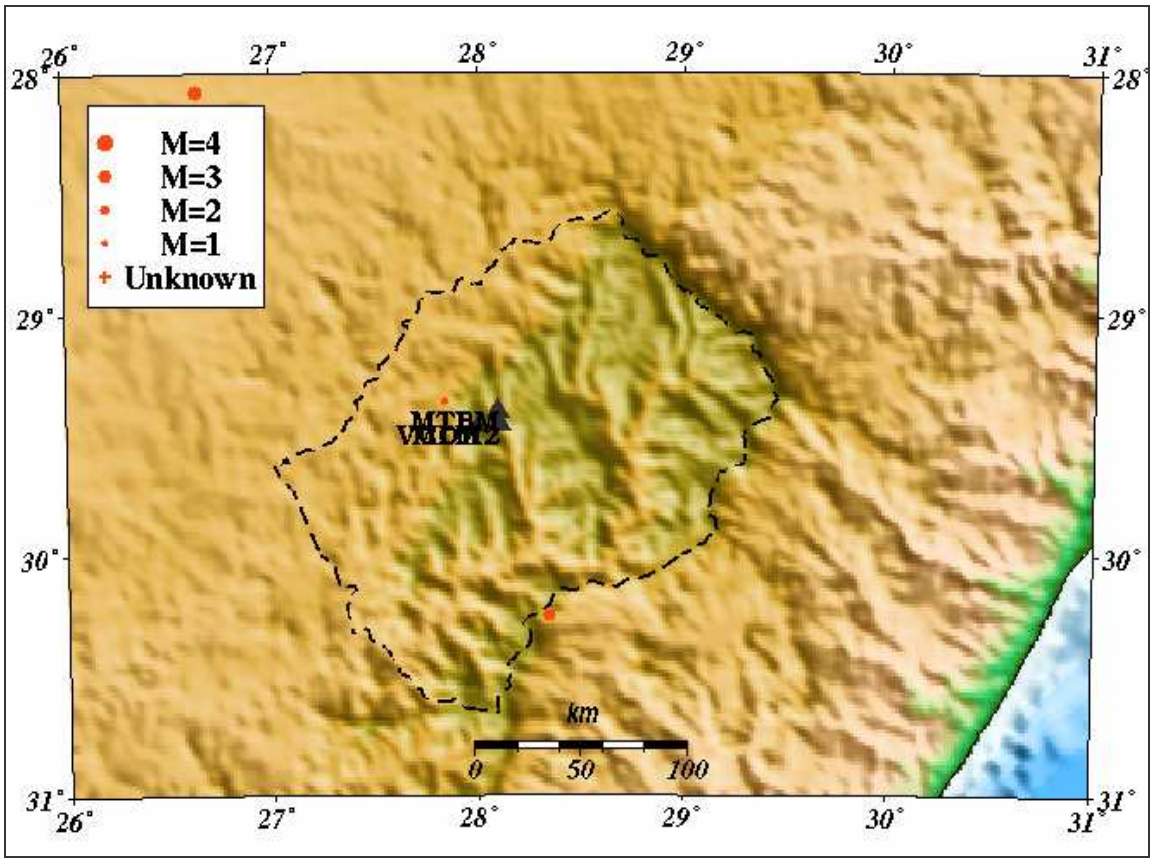

Figure 4.3: A map of the earthquakes for which moment magnitude was calculated.

4.3. Induced Seismicity

Reservoir Induced Seismicity (RIS) was first experienced in Lesotho after the implementation of the Lesotho Highlands Water project in 1995. Prior to this, there had not been any seismic monitoring and all the information regarding earthquake occurrences is documented mostly by the Council for Geosciences, South Africa. In his thesis work, Brandt (2000) reviewed the seismicity at the Katse dam, which is the main storage dam for the period 1995 to 1999. The maximum earthquake recorded has magnitude M_L = 3.0 (M_C = 3.2) and occurred 5 km upstream of the dam, on January 3, 1996. This event resulted in a1.5 km long rupture zone caused damage to several houses in its vicinity.

The results from Brandt (2000) indicate that coda magnitudes (M_C) are generally larger than local magnitudes M_L and magnitudes were complete for M_C = 1.2.

Seismicity at Katse dam diminished with time after impoundment was complete and from the data used in this study there is no significant RIS recorded. A new network installed at the Mohale dam, which is a subsidiary feeding into the main dam, has not recorded any RIS. Figure 4.4 is a map of reservoir induced seismicity.

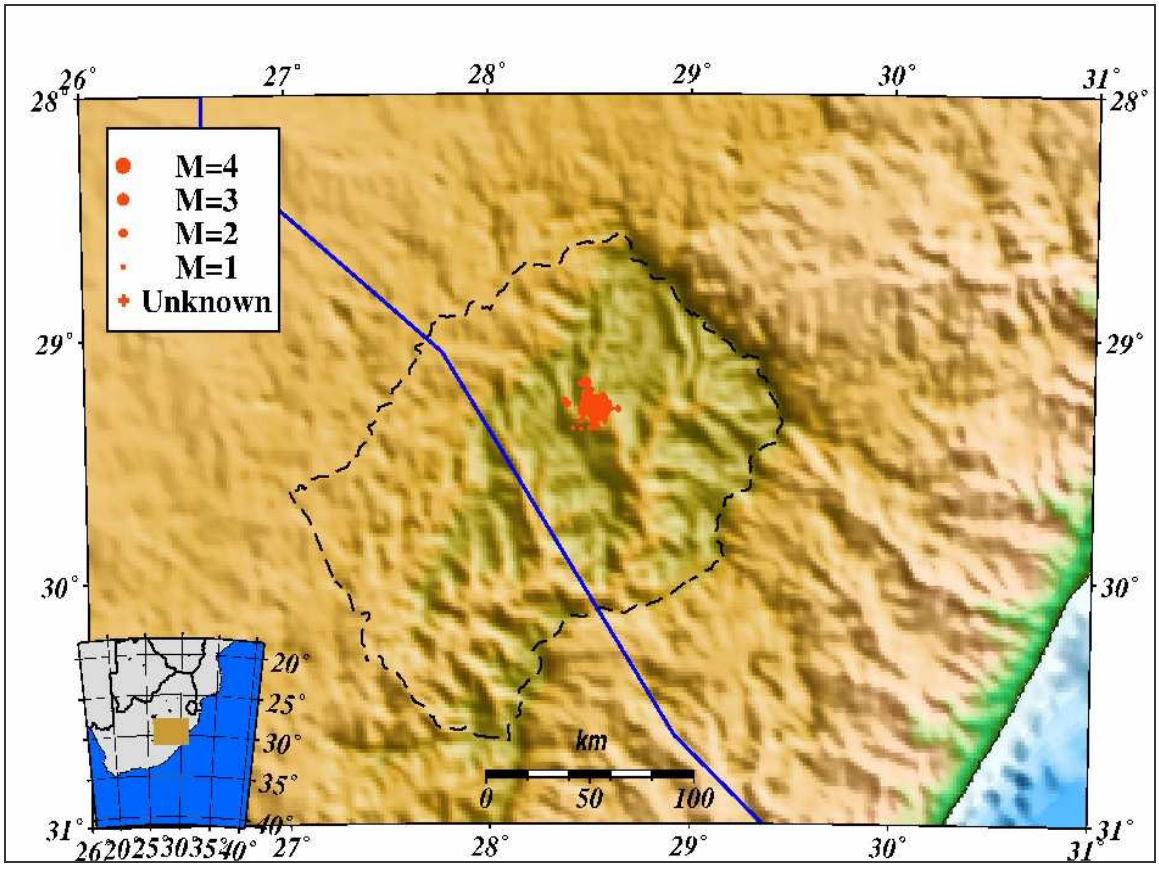

Figure 4.4: Map showing reservoir induced seismicity. Data from Brandt (2000).

5 Hazard of Lesotho

This chapter is a description of the preliminary Seismic Hazard Assessment (SHA) carried out for purposes of this thesis. As mentioned in chapter 1, an SHA has never been made for the country and with the number of dams envisaged for the LHWP, it was found necessary to conduct one. In addition, Lesotho has experienced five earthquakes of magnitude $M_L > 4.0$ between 1966 and 2002.

There are two different methods that can be used in preparing a seismic hazard analysis; namely the Deterministic Seismic Hazard Assessment (DSHA) and Probabilistic Seismic Hazard Analyses (PSHA). Depending on the area of interest, sources associated with seismicity in a region and reasons for the need of a hazard analysis - which could vary from engineering purposes to designing seismic codes for a country – one could decide to use either method.

In this analysis, a Probabilistic Seismic Hazard Analysis (PSHA) using a Poisson Model will be described with reference to this study. The first task is to describe the earthquake sources zones then the seismicity recurrence for each source and finally estimate the effects the earthquakes will have. The results of the investigation are shown as contour plots showing maximum expected ground motion for a given return period.

In order to do all of the above a seismic catalogue is prepared, from which earthquake source zones are defined.

5.1 Catalogue Preparation

The catalogue used in this study covers the period 1854 to 2006 and the region bounded by the following coordinates: 31^0 S to 28^0 S and 26^0 E to 31^0 E. This is done so as to account for seismicity occurring outside the borders of Lesotho; but which could have an effect on the country.

The catalogue is compiled from earthquake data sets from three main sources, namely:

i) The Lesotho Highlands Water Project (LHWP),

ii) South African Council for Geoscience (CGS),

iii) The International Seismological Center (ISC).

A brief description of the data sources is given in section 5.1.1.

5.1.1 Data Sources

i) LHWP data

Parametric data from the Lesotho Highlands Water Project for the period 1995 to January 2001 was obtained from previous work that was done in collaboration with the Council for Geosciences, South Africa. Part of this data is compiled in previous thesis work (Brandt, 2000) and is for the period 1995 to 1999. Additional data from the Lesotho Highlands Water Project (LWHP) that was re-analysed for purposes of this thesis spans from February 2002 to December 2006. This data includes waveform files.

ii) South African Council for Geoscience data

The South Africa Seismic network had its first seismograph installed in 1910 and a more modern network has gradually developed since 1971 . Historical seismicity for southern Africa dates as far back as 1620 and is reported in terms of intensity and magnitudes up to 1970, in the CGS databank. The first event for the study region was recorded in 1854. This parametric data was obtained through personal communication with the CGS personnel (Saunders, 2007).

iii) International Seismological Centre data

This data is sourced from the International Seismological Centre's (ISC) database, which is a non-governmental institution funded by interested academies compiling earthquake information from all over the world. The data is parametric and covers the period 1904 to 2006; however, the first seismic event of the region of study was recorded in 1957.

5.1.2. Catalogue clean-up and merging

In order to investigate the seismic activity for a background study of the entire southern African region as well as compute the seismic hazard for the study region, the three datasets described in section 5.1.1 have been merged together to produce a single catalogue. This data is organized into one database in Nordic format and analyzed with the SEISAN software (Havskov and Ottemöller, 2005). All programmes used, from compiling the catalogue to computing the hazard, are described in appendix B.

The two LHWP datasets were merged together with ease since there was no overlap. In merging all the other datasets, there were overlaps and therefore a catalogue clean-up was made in order to take care of the duplicates. The criteria for this clean-up was set up by considering factors like the number of stations that an event was recorded by or the proximity of the epicentral location to either of the reporting agencies. Based on these criteria, the best solutions are considered and kept as parent events while the overlapping (duplicate) events are appended to the parent events, such that all information pertaining to that particular event is kept. After the clean-up, there is a total of 2636 events in the database, covering the period from April 1620 to December 2006 and 1265 of these are located within the study region. Of these 1265 earthquakes, 59 are removed in the hazard computation since they are associated with blasting activities.

5.1.3. Magnitude unification

Different agencies report different magnitude types hence it is important to have a catalogue with a homogeneous set of magnitudes, once the catalogue compilation is done. The main aim of unifying magnitudes is to average out uncertainties between the different types, by a least squares regression plot method.

In this study, the relations between the different magnitude types in the catalogue are calculated using the SEISAN program called MAG (Havskov and Ottemöller, 2005), which is described in Appendix C. However, the unification was impractical as there

were too few points over which to make a comparison and therefore the catalogue is left with its different magnitude types reported.

Since majority of the earthquakes have been reported with M_L (see Tables 4.1 and 5.1), the rest of the computations are made with the use of this magnitude, irrespective of the reporting agency.

Table 5.1: Distribution of the different magnitudes in this study's catalogue. Some events are reported with more than one magnitude type.

Magnitude type	Number of earthquakes	Total number of earthquakes
M_L	991	1206
M_b	115	
M_C	91	
M_S	6	
M_W	3	

5.1.4. Data completeness

The catalogue completeness for the period after 1850 to around 1950 is for magnitude $M_L \geq 3.0$. After the 1950's the increase in seismicity could also be attributed to the mining activities in South Africa. The implementation of the Worldwide Standardized Seismographic Network in the early 1960's and the South African Seismic Network in the early 1970's, respectively, could also be the reason that more seismicity is evident after these times. The period 1996 to early 2000's is marked by an increase in reservoir-induced seismicity with some events having magnitudes less than zero. As mentioned in chapter 3, the LHWP installed its seismic network in 1995 thereby rendering an even better coverage for recording earthquakes in Lesotho. Figures 5.1 and 5.2 show the yearly statistics of the earthquake catalogue and the magnitudes distribution, respectively.

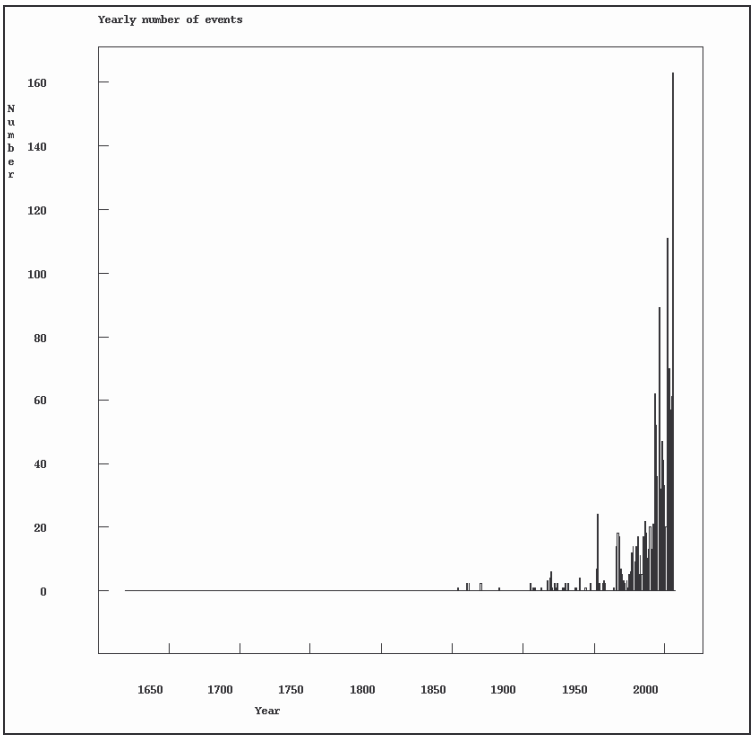

Figure 5.1: A yearly statistics of the earthquakes in the catalogue used for purposes of this thesis. The first seismic record is observed after 1850. After 1900 the activity begins to increase slightly. Around 1950 another increase is seen and around 1990 there is an even bigger increase.

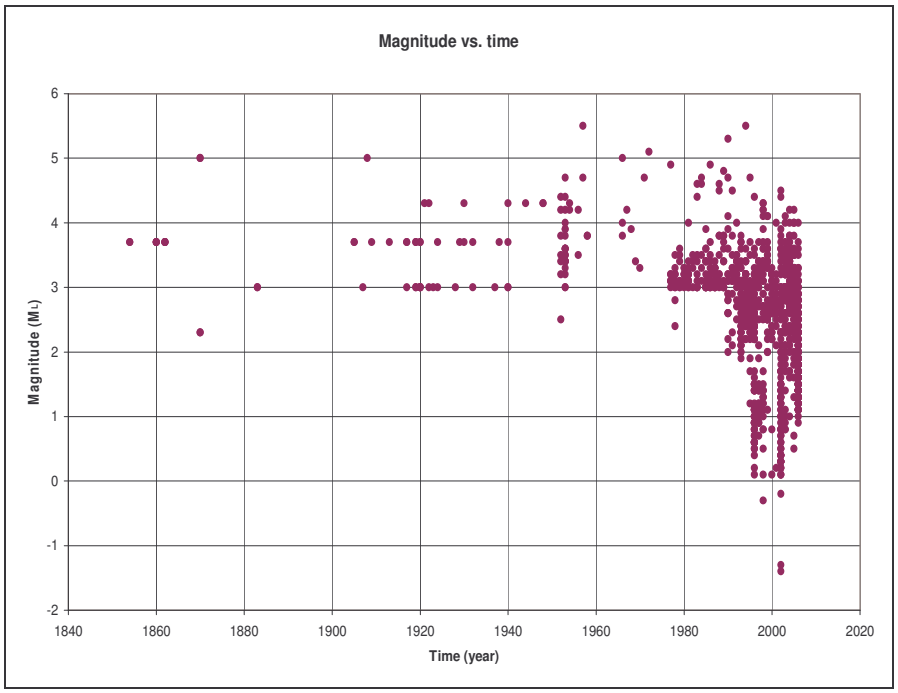

Figure 5.2: Magnitude distribution of the compiled catalogue for the study region. The catalogue is complete for ML around 3.8 up to 1870; complete for ML = 3.0 up to 1965 and from 1996 to 2006 the catalogue completeness is for very small events (ML < 1).

5.2 Probabilistic Seismic Hazard Analysis (PSHA) Method

The PSHA method is used in this study, since it is the best for regions of low seismic activity as opposed to the DSHA, which requires thorough knowledge of faults in an area. The PSHA method integrates a wide range of information, which can either be multi-valued or a continuous set of events and takes into account model and uncertainties in parameters used during analysis (Chen et al., 1998; Reiter, 1990).

The PSHA uses Poisson Model which assumes that sources have no memory of past records. This means all earthquakes are independent of each other and can happen at any time or place within a source zone.

The procedure for conducting a PSHA comprises 4 main steps modified from a procedure described by (Cornell, 1968) and reiterated by (Reiter, 1990). The first 3 steps are used as input parameters. The procedure is illustrated by figure 5.3.

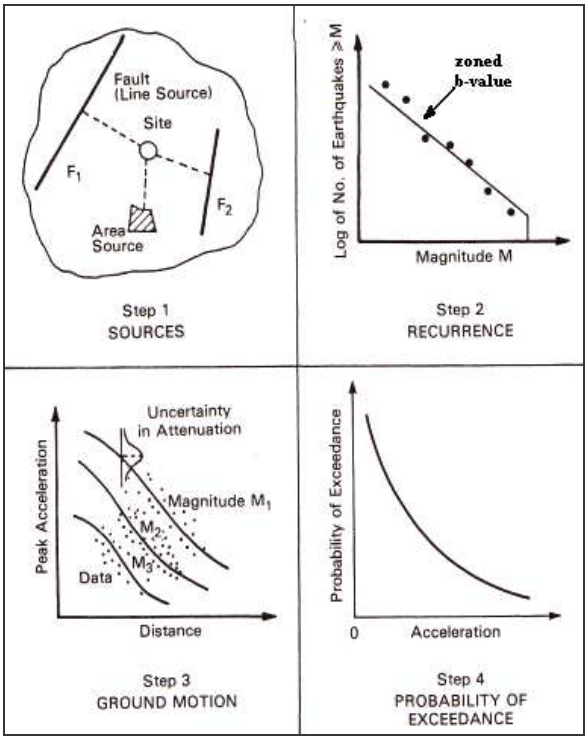

Figure 5.3: Basic procedure for seismic hazard assessment (Chen et al., 1998; Reiter, 1990).

First, the region of Lesotho is divided into five seismic source zones and then the seismicity of each zone is characterized by several parameters. These parameters include an annual occurrence rate, b-value, and a lower and upper bound magnitude for the Gutenberg-Richter (G-R) relation (which is defined in equation 2).

$$\text{Log}(N) = a - bM \qquad (2)$$

where N is the number of earthquakes of a given magnitude M, or larger, expected to occur during a specified period of time. "a" is the logarithm of the number of earthquakes of magnitude $M \geq 0$, expected to happen during the same time. (Reiter, 1990) describes "a" as "an activity rate whose size depends on the overall earthquake occurrence." "b" is the slope of the curve, which characterizes the distribution of small to large earthquakes and is termed the b-value.

Since earthquakes can happen anywhere in a source zone, the distances from all locations in the zone should be considered by estimating earthquake effects. This requires knowledge of the area's ground motion attenuation since it is dependent on the size of the earthquake. In the third step the earthquakes effects in the sources are estimated based on the attenuation table by SPU97.PRN (Spudich et al., 1997) modified by (Ojeda, 2007) which is described briefly in section 5.3.3. Finally, the seismic effect for the region is obtained by integrating the seismic effects contributed by the individual source zones and the probability distribution is incorporated in the analysis to depict the maximum ground motion at a certain probability of exceedance, for a specific duration of time.

Evaluation of several attributes for each source zone is required in order for the PSHA to be valid. These include:

1) Evaluation of the earthquake activity rate (number of earthquakes per year),
2) Evaluation of the catalogue completeness (threshold magnitude),
3) Identification of and upper bound magnitude (maximum magnitude),
4) Estimation of the maximum expected magnitude.

5.3 Input for Probabilistic Seismic Hazard Analysis

5.3.1. Seismic Sources

The definition of a source zone is based on geological, geophysical or seismological data interpretation. A source zone is a configuration within which earthquakes are observed to occur at the same rate with respect to magnitude irrespective of their location (Reiter, 1990). The study region has been divided into 5 source zones, delineated as polygons, namely:

i) South African mines
ii) Senqu Seismic Belt zone
iii) North Lesotho
iv) Drakensberg
v) Katse

These source zones are illustrated in figure 5.4.

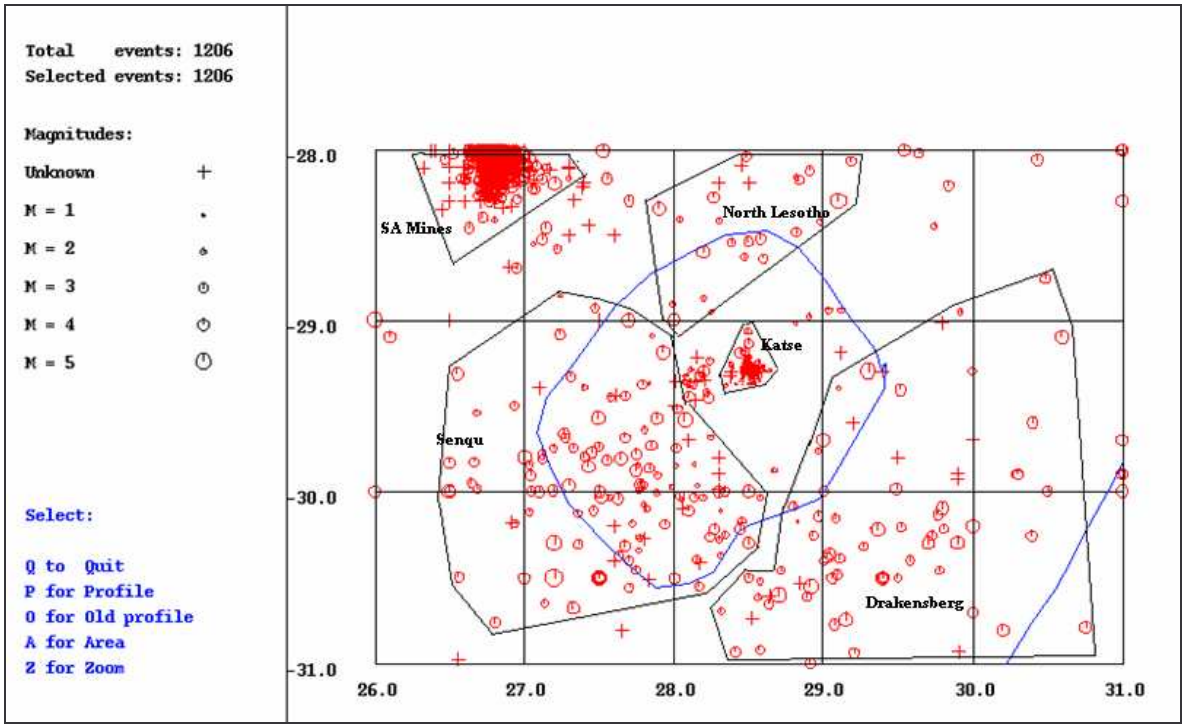

Figure 5.4: Epicentral map of Lesotho with the source zones outlined in black.

From figure 2.4, which shows the main geological structures of the study region, it is aparent that the seismicity of Lesotho is concentrated more in the southern part and follows the Senqu seismic belt as described by(Hartnardy, 1998). The Senqu Seismic Belt has a north-west to south-east trend cutting across the country in the same manner. It is along this belt that some scientists have proposed a model indicating the southern propagation of the EARS into the Indian ocean (Bird, 2003; Hartnady, 2002).

In the northern part of the country, there are structural features which also could be attributed to the occurrence of earthquakes, however, reservoir induced seismicity characterizes the central part.

5.3.2. Recurrence relations

The recurrence relationship is given such that there is no controlling earthquake in a zone. This relationship indicates a chance of occurrence for an earthquake of a certain size (i.e. magnitude) in a given time period. The recurrence relationship is determined by a logarithmic function given in equation (2). Figure 5.5 shows a plot of the Gutenberg-Richter (G-R) relation for the study region and the parameters used to generate the plot. Individual source zone b-value plots are in appendix E.

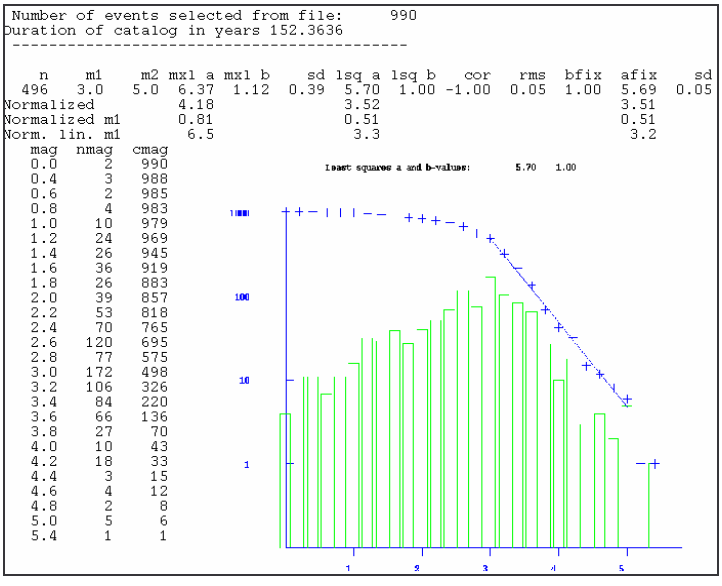

Figure 5.5: b-value plot for the study area. The magnitude step used is 0.2 and the a- and b-values are 5.70 and 1.00 respectively and Output file showing the parameters used in the b-value plot.

5.3.3. Attenuation

Since the events are assumed to happen anywhere in a source zone, the distances from all locations in the zone should be considered and estimating the effect of an earthquake can do this. This requires the knowledge of the area's ground motion attenuation, which can be determined from ground motion curves and/or standard attenuation tables from studies made worldwide. The ground motion is dependent on the size of the earthquake magnitude; therefore the attenuation curves/tables are given for a specific magnitude and hence are functions of both distance and magnitude. The ground motion is measured in peak ground acceleration.

There are several attenuation tables made for different regions in the world describing the ground motion changes in relation to the distance from the epicentre. The attenuation model is a vital tool since it controls the output ground motion. Since there is no attenuation table/model for Lesotho, the model used in this study is the SPU97.PRN (Spudich et al., 1997). This model consists of a description of normal faults in solid rock regions worldwide and since Lesotho is situated on the stable African plate, with focal mechanisms of normal fault nature, this seemed the best to use. Other tables were not considered due to their emphasis on either strike slip faults or soft soil and were more localized for Europe.

5.3.4. Input Parameters

The seismic hazard is computed by the use of the CRISIS99 program, which is described in appendix B. The input file required, for the program to run, includes information regarding the location of the area of interest, the coordinates for the defined source zones, the recurrence periods chosen and the a- and b-values. This program yields three output files, containing summary of calculations at each grid; identification header and exceedance rates for the type and level of intensity; as well as a map with intensity levels for fixed return periods and coordinates for each zone. This map is used as input for plotting the hazard results. Table 5.2 lists the input parameters used in running the CRISIS99 program.

Table 5.2: Input parameters used by the CRISIS99 program to calculate the seismic hazard. Thr b-value indicates the XX ans the activity rate is the exceedance of the threshold magnitudes in events/year.

Zones	$M_{Threshold}$	$M_{Observed}$	$M_{Expected}$	b-value	Activity rate	Time Span
Background	3.0	5.5	6.0	1.00	6.513	152
Drakensberg	3.0	5.0	5.5	0.84	0.479	146
North Lesotho	3.0	5.0	5.5	0.84	0.390	136
SA mines	3.0	4.8	5.6	1.28	9.423	52
Senqu	3.0	5.5	6.0	0.91	1.049	123
Katse		3.2	3.7	0.51	0.9	10

The threshold magnitude ($M_{Threshold}$) is M_L = 3.0 and is the lower bound magnitude used in this study, since the catalogue was complete for magnitude 3 for most years. The observed magnitude ($M_{Observed}$) is the maximum observed magnitude in a source zone and the expected magnitude ($M_{Expected}$ is $M_{Observed}$ + 0.5). The b-value is a characterization of small to large earthquakes on the Gutenberg-Richter (G-R) plot. As it is shown in table 5.2, the activity rate is the number of earthquakes per year and the time span is the number of years of earthquake records, for a given source zone.

5.4 Probabilistic Seismic Hazard Analysis and Results

The calculated values for the seismic hazard are given as peak ground acceleration (PGA) by the CRISIS99 program and are computed for 5 return periods.

5.4.1. Return periods

Return periods are the core of the actual seismic hazard analysis and provide a tool for incorporating descriptions of the whole earthquake history in a region. When computing the hazard using the probabilistic method, the effects of all earthquakes with different magnitudes occurring in different places, in the different zones, with different

probabilities should be taken into account. The hazard for a specific time (return period), RP, is given by:

$$RP = \frac{-T}{\ln(1 - P(Z > z))} \tag{3}$$

where T is the period of interest and P(Z>z) is the desired probability of exceedence during time T. A standard return period that is considered worldwide is 475, corresponding to a 10 % probability of exceedance of a certain magnitude, for a 50-year lifetime.

The return periods chosen for this study are based on a 10% probability and and are shown in table 5.3.

Table5.3: A list of the return periods used in this seismic hazard analysis, with corresponding probability of exceedance and time period.

Return Period	Time (Years)	P(Z>z)
100	10	0.1
200	21	0.1
475	50	0.1
1000	105	0.1
50000	500	0.1

The standard formulation of PSHA is to calculate the frequency of exceedance of ground motion amplitude by an equation the of the following form (McGuire, 1995)

$$\mathrm{E(z)} = \sum_i \alpha_i \iint f_M(m) f_R(r) \cdot P(Z > z \mid m, r) \cdot dmdr \tag{4}$$

where E(z) is the expected number of exceedances of ground motion level z during a time period; α_i is the activity rate for source i; $f_M(m)$ is the recurrence relation in source i while $f_R(r)$ is the probable distribution of the source distance between the different locations in the source i and the site for which the hazard is being estimated. $P(Z > z \mid m, r)$ is the probability that a given earthquake of magnitude m and epicentral distance r will exceed ground motion.

5.4.2 Hazard Results

The seismic hazard maps computed represent the 5 different periods discussed in 5.3. Since the 475 year return period is the most significant, figure 5.4 shows the hazard of the study area with respect to this return period. Other maps are shown in appendix G

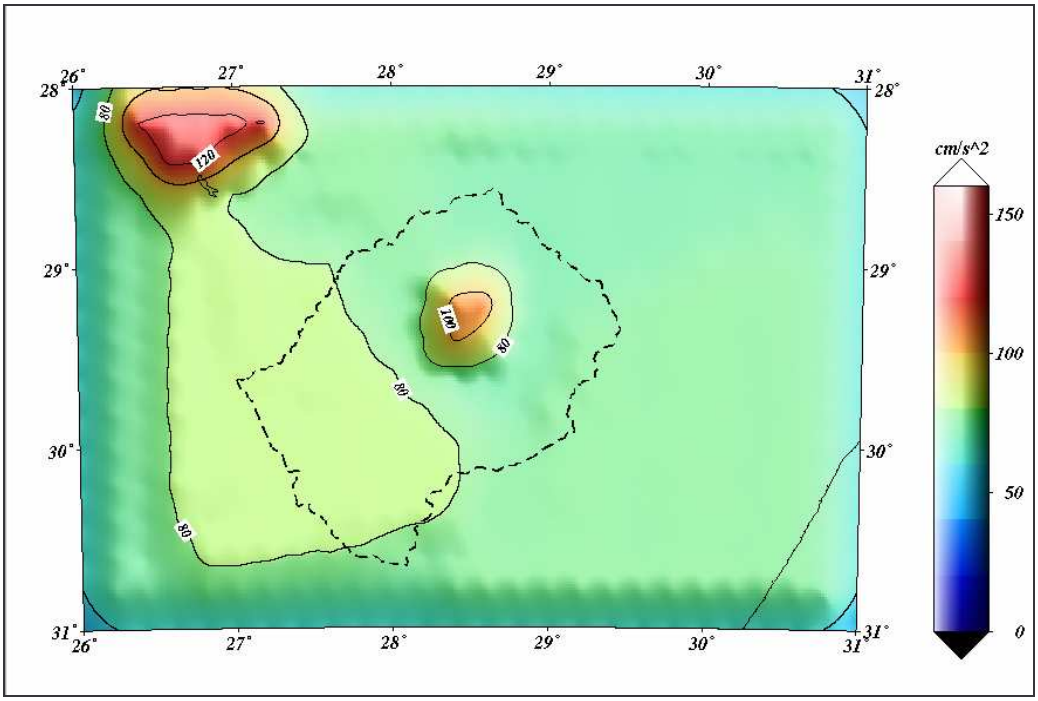

Figure 5.6: Seismic Hazard map for Lesotho region for a return period of 475 years. This map represents a 10% probability of exceedance in 50 years. The unit for ground motion is cm/s^2 . The attenuation table used use the SPU97.PRN.

The results are as expected since there is a generally low level of seismicity in the region. The mines region exhibit the highest level of hazard as expected, with peak ground acceleration (PGA) of 120 cm/s^2 (i.e. 0.12 g). The LHWP area shows a maximum PGA of 100m/s^2 while the Senqu Seismic zone has 80 cm/s^2 as the maximum PGA.

As the return period increases the hazard also increases and this is expected. Considering the mines region, which has the highest level of hazard, a return period of 100 years yields a maximum PGA of 100 cm/s^2 (i.e. 0.1 g), while a 5000-year return period corresponds to a maximum PGA of 200 cm/^{2} (0.2 g).

A comparison of the obtained results was made with results from the South African Council for Geoscience, where seismic hazard maps were produced for a 10% probability of exceedance and spectral acceleration of 10 Hz at least once in 50 years (Kijko et al., 2003). Figure 5.7 is a map of the calculated hazard for South Africa indicating that the study region has a fairly low level of hazard.

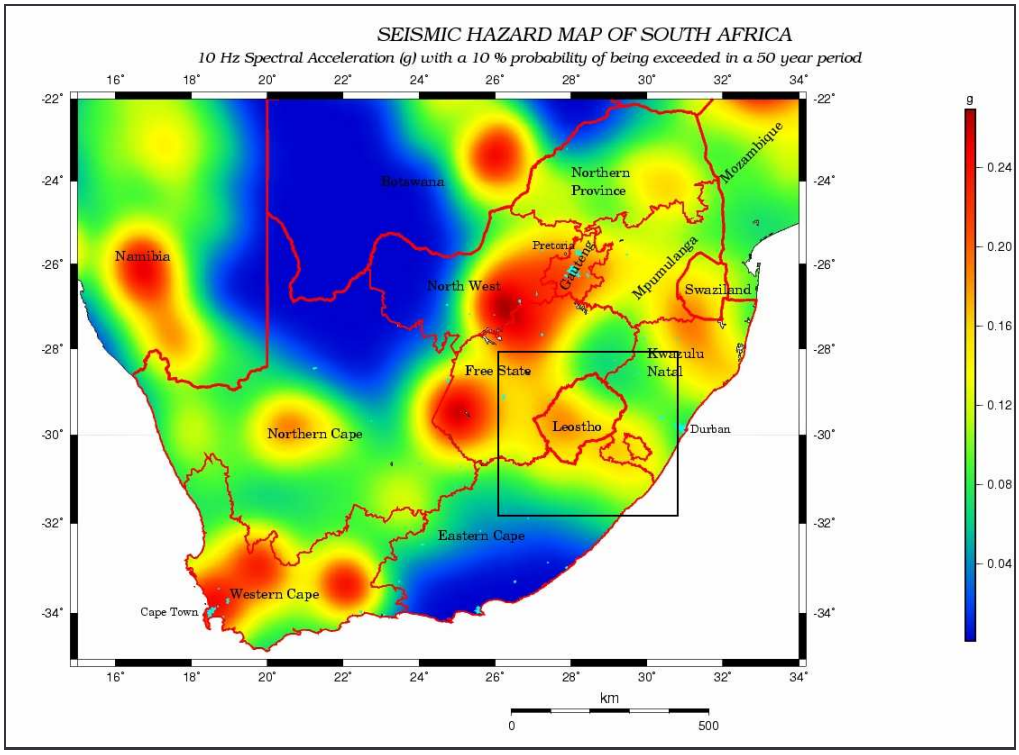

Figure 5.7: Probabilistic Seismic Hazard Map of South Africa for a 50-year period by Kijko et al, (2003). The study area is outlined with the black box. The 10 Hz spectral acceleration in the study region is in the range 0.12 g to 0.2 g.

6 Discussion and Conclusion

In this thesis, a comprehensive earthquake catalogue has been produced for Lesotho, from which the seismicity and seismic hazard of the region are studied. This catalogue is put together from earthquake information obtained from 3 main sources; Lesotho Highlands Water Project (LHWP), Council for Geoscience (CGS) and International Seismological Center (ISC). The datasets from all sources are merged to produce a single catalogue which is cleaned and known explosions are removed. The catalogue spans from 1854 to 2006 and has 1206 earthquakes.

There is a significant amount of data missing from the LHWP dataset when comparing to the ISC data. This is attributed to the following factors

- Stations's downtimes
- Inadequacy in the detection capability
- Timing problems
- The criteria used for extracting data for compiling the catalogue

Coda Q calculation were made and based on this moment magnitude was calculated for the best events, however in the study region there were only 3 events. As a result the magnitudes were not converted and M_L was used throughout this study.

The distribution of earthquakes within Lesotho is more concentrated in the southern part, where it is in line with geologic features (e.g lineaments) and seems to be related to the general tectonics in the area. The distribution of earthquakes is aligned with the Senqu Seismic Belt and seems to accommodate the postulation of a possible plate boundary, supporting the extension of the East African Rift System.

A preliminary probabilistic seismic hazard assessment for Lesotho is made on the basis of the compiled catalogue. The region has been divided into 5 zones and recurrence relations for the different zones are computed.

It was difficult to convert the different magnitudes to one, therefore this step was omitted. Since there are a large number of earthquakes reported with local magnitude M_L, this is the magnitude type used throughout the hazard computations. The attenuation table used is the SPU97.PRN (Spudich et al., 1997), which is suitable for normal faults and solid rock regions worldwide. Though the threshold magnitude is usually set to 4.0 when computing seismic hazard, in this study, it has been set to 3.0 since an earthquake of that size has caused significant damage in the region.

As expected, the results indicate that the mines' area has the highest hazard, followed by the Katse dam area. For a return period of 475 with a 10 % probability of exceedance, the maximum expected peak ground acceleration (PGA) is 0.12 g in the mines region. These results are in accordance with previous hazard studies(Kijko et al., 2003).

Reservoir and mine induced seismicity are not natural and therefore, their influence in the hazard should be treated with caution. Ideally, these should have been excluded in the hazard computations; however they have been included so as to show their influence on the hazard of the region.

The results obtained from this study indicate that there is a need for future studies in the region. The methods used from extracting the data to running the hazard should be revised. The current seismic network problems should be investigated and therefore addressed accordingly.

Since a realistic seismic hazard assessment highly depends upon the understanding of fault characteristics, future hazard work will require extensive work in this regard. For hazard computations, it would be more meaningful to select zones in accordance with known faults or lineaments. A better understanding of the relation between the Senqu Seismic Belt and the possible extension of the East African Rift System is required.

7 Acknowledgements

I would like to express my sincere gratitude to a number of people who have supported and guided me during my studies.

First, I would like to thank my supervisors, Jens Havskov and Kuvvet Atakan for their supervison, valuable discussions and an excellent environment they provide for their students. Keep up the good work!

A special thanks to the Norwegian State Loan Fund for granting me the support to pursue my studies and to my employer, the Lesotho Highlands Development Authority for granting me study leave.

I am greatly indebted to Mohammed Raeesi for the hours he spent guiding and helping me understand the Global Mapping Tools (GMT) programme which is used in plotting most of the maps produced in this thesis. To Louise Bjerrum and Aleksandre Kandilarov thanks for your invaluable assistance during critical times. I wish to thank Berit Marie Storheim and Annelise Kjærgaard for coming to my rescue when my supervisors were not around. Thanks to Øyvind Natvik who has always helped solve my computer problems. To Zoya Zarifi, Alrasheed Warage, Asude Arsalan, the words of encouragement I have received from you have always been inspiring.

To my friends (both old and new), thank you for supporting my efforts and always being there for me in the toughest of time, in particular, Uopo Njaula, Palesa Moonyane and Nancy Motebe.

Finally, I would like to thank my family. My mother - ‘Mapheko Motsieloa for being a pillar of strength; my husband - Malephane Malephane for being a great friend and my sons ‘Mile and T’sepang for understanding that mummy had to study. Thank you all, I am truely grateful.

8 References

Aki, K., and Chouet, B., 1975, Origin of coda waves, Source, Attenuation and Scattering effects: *Journal of Geophysica Research*, v. 80, p. 3322-3342.

Aranda, C., 2000, A short user's manual for GBV-316 digital seismograph, Volume 1: Bergen, Institute of Solid Earth Physics, University of Bergen, p. 1-8.

Asl, A., 2000, GeoSIG GBV-116/316(W) Operation Manual: Glattbrugg, GeoSIG Ltd, Switzerland.

Bertil, D., and Regnoult, M., 1998, Seismotectonics of Madagascar: *Tectonophysics*, v. 294, p. 57-74.

Bird, P., 2003, An updated digital model of plate boundaries: *Geochemistry, Geophysics, Geosystems (G^3)*, v. 4, p. 1-52.

Brandt, M.M.B.C., 2000, A Review of the Reservoir Induced Seismicity at the Katse Dam, Kingdom of Lesotho, November1995 to March 1999 [Master thesis]: Bergen, **University of Bergen**.

Chen, Y., Liu, J., Chen, L., and Chan, L.S., 1998, Global Seismic Hazard Assessment Based on Area Source Model and Seismicity Data: Natural Hazards, v. 17, p. 251-267.

Chu, D., and Gordon, R.G., 1999, Evidence for motion between Nubia and Somalia along the Southwest Indian ridge: *Nature*, v. 398, p. 64-67.

Cornell, C.A., 1968, Engineering seismic risk analysis: Bulletin of the Seismological Society of America, v. 58, p. 1583-1606.

DeMets, C., Gordon, R.G., Argus, A.F., and Stein, S., 1990, Current Plate motions: *Geophysical Research Letters*, v. 21, p. 2191-2194.

Doucouré, C.M., deWit, M.J., and Mushayandebvu, M.F., 1996, Effective thickness of the continental lithosphere in South Africa: *Journal of Geophysica Research*, v. 101, p. 11,291-11,304.

Fenton, C.H., and Bommer, J.J., 2007, The M_w 7 Machaze, Mozambique Earthquake of 23 February 2006: Seismological Research Letters, v. 77, p. 426-439.

Gordon, R.G., and Stein, S., 1992, Global Tectonics and Space Geodesy: *Science*, v. 256, p. 333-342.

Hartnady, C.J.H., 2002, Earthquake hazard in Africa: perspectives on the Nubia-Somalia boundary: *South African Journal of Science*, v. 98, p. 425-427.

Hartnardy, C.J.H., 1998, Lesotho Seismotectonics, *Unpublished Manuscript*.

Hattingh, E., and Pretorius, J.V.L., 2004, Station Book for the Mohale Telemetered Seismograph Network (MTSN): Pretoria, Council for Geoscience.

Hattingh, E., Pretorius, J.V.L., and Saunders, I., 2004, Station Book for the Katse Telemetered Seismograph Network (KTSN): Pretoria
Council for Geoscience.

Havskov, J., and Alguacil, G., 2004, Instrumentation in Earthquake Seismology, Springer.

Havskov, J., Malone, S., McClurg, D., and Crosson, R., 1989, Coda Q for the State of Washington: *Bulletin of Seismological Society of America*, v. 79, p. 1024-1038.

Havskov, J., and Ottemöller, L., 2005, SEISAN: The Earthquake Analysis Software: Bergen, University of Bergen.

Horner-Johnson, B.C., Gordon, R.G., Cowles, S.M., and Argus, D.F., 2005, The angular velocity of Nubia relative to Somalia andthe location of the Nubia -Somalia-Antarctica triple junction: *Geophysical Journal International*, v. 162, p. 221-238.

Hough, S.E., Seeber, L., and Armbruster, J.G., 2003, Intraplate Triggered Earthquakes: Observations and Interpretation: *Bulletin of Seismological Society of America*, v. 93, p. 2212-2221.

Jacobs, J., and Thomas, R.J., 1994, Oblique collision at about 1.1 Ga along the southern margin of thr Kaapvaal Continent, south-east Africa: *Geol Rundsch*, v. 83, p. 322-333.

Jacobs, J., Thomas, R.J., and Weber, K., 1993, Accretion and indentation tectonics at the southern edge of the Kaapvaal craton during the Kibaran (grenville) orogeny: *Geology*, v. 21, p. 203-206.

James, D.E., 2003, Imaging crust and mantle beneath southern Africa: The southern Africa broadband seismic experiment: *The Leading Edge*, v. 22, p. 238-249.

James, D.E., and Fouch, M.J., 2001, Formation and Evolution of Archean Cratons: Insights from Southern Africa: *Submitted to Geological Society for inclusion in Special Publication: Early Earth*.

James, D.E., Niu, F., and Rokosky, J., 2003, Crustal Structure of the Kaapvaal craton and its significance for early crustal evolution: *Lithos*, v. 71, p. 413-429.

Johnston, A.C., 1996, Seismic moment assessment of earthquakes in stable continental regions - III. New Madrid 1811-1812, Charleston 1886 and Lisbon 1755: *Geophysical Journal International*, v. 126, p. 314-344.

Kanamori, H., and Anderson, D.L., 1975, Theoretical basis of some empirical relations in seismology: *Bulletin of the Seismological Society of America*, v. 65, p. 1073-1095.

Kijko, A., Graham, G., Bejaichund, M., Roblin, D., and Brandt, M.B.C., 2003, Probabilistic Peak Ground Acceleration and Spectral Seismic Hazard Maps for South Africa: Pretoria, *Council for Geoscience*.

Kijko, A., Retief, S.P.J., Graham, G., and Bejaichund, M.S., 2002, Seismic Hazard and Rsik Assessment Based on the Parametric-Historic Procedure. Case Study:Tulbagh, South Africa: Pretoria, Council for Geoscience, p. 1-39.

Lay, T., and Wallace, T.C., 1995, Modern Global Seismology Academic Press.

McClusky, S., Balassanian, S., Barka, A., Demir, C., Ergintav, S., Georgiev, I., Gurkan, O., Hamburger, M., Hurst, K., Kahle, H., Kastens, K., Kekelidze, G., King, R., Kotzev, V., Lenk, O., Mahmoud, S., Mishin, A., Nadariya, M., Ouzounis, A., Paradissis, D., Peter, Y., Prilepin, M., Reilinger, R., Sanli, I., Seeger, H., Tealeb, A., Toksöz, M.N., and Veis, G., 2000, Global Positioning System constraints on plate kinematics and dynamics in the eastern Mediterranean and Caucasus: *Journal of Geophical Research*, v. 105, p. 5695-5720.

McGuire, R.K., 1995, Probabilistic seismic hazard analysis and design earthquakes: Closing the loop: *Bulletin of the Seismological Society of America*, v. 85, p. 1275-1284.

Mellis, L.M.J., and Chavellier, L.P., 2000, On the origin of seismicity in Southern Africa, Paleoseismology Workshop: Stellenbosch, South Africa.

Mitchell, B.J., 1981, Regional variation and frequency dependence of Q{beta} in the crust of the United States: *Bulletin of the Seismological Society of America*, v. 71, p. 1531-1538.

Mitha, V.R., 2006, An insightinto magma supply to the Karoo Igneous Province: a geochemical investigation of Karoo dykes adjacent to the Northwestern sector of the Lesotho volcanic remnant [Master thesis]: Grahamstown, **Rhodes University**.

Musson, R.M.V., 2004, A critical history of British Isles earthquakes: *Annals of Geophysics*, v. 47.

Nguuri, T.K., Gore, J., James, D.E., Webb, S.J., Wright, C., Zengeni, T.G., Gwavava, O., Snoke, T.A., and Group, K.S., 2001, Crustal structure beneath southern Africa and its implications for the formation and evolution of the Kaapvaal and Zimbabwe cratons: *Geophysical Research Letters*, v. 28, p. 2501-2504.

Odum, K.J., J., S.W., Shedlock, K.M., and Pratt, T.L., 1998, Near-surface structural model for deformation associated with the February 7, 1812, New Madrid, Missouri earthquake *Geological Society of America*, v. 110, p. 149-162.

Ojeda, A., 2007, SPU97.PRN Attenuation table.

Reiter, L., 1990, Earthquake Hazard Ananlysis: Issues and Insights: New York, Columbia University Press.

Roecker, S.W., Tucker, B., King, J., and Hatzfeld, D., 1982, Estimates of Q in central Asia as a function of frequency and depth using the coda of locally recorded earthquakes: *Bulletin of the Seismological Society of America*, v. 72, p. 129-149.

Rudolf, M., 2002, Piece of the tectonic puzzle found: Geotimes, p. 1-2.

Saunders, I., 2007, Historical Earthquakes' List for Southern Africa, *personal communiation*.: Pretoria, Council for Geoscience.

Silver, P.G., Gao, S.S., Liu, K.H., and Group, K.S., 2001, Mantle deformation beneath southern Africa: *Geophysical Research Letters*, v. 28, p. 2493-2496.

Singh, S.K., Rodriguez, M., and Esteva, L., 1983, Statistics of small earthquakes and frequency of occurrence of large earthquakes along the Mexican subduction zone: *Bulletin of the Seismological Society of America*, v. 73, p. 1779-1796.

Spudich, P., Fletcher, J., Hellweg, M., Boatwright, J., Sullivan, C., Joyner, W., Hanks, T., Boore, D., McGarr, A., Baker, L., and Lindh, A., 1997, SEA96-A new predictive relation for earthquake ground motions in extensional tectonics regimes: *Seismological research letters*, v.68 .

Stein, S., and Wysession, M., 2003, Introduction to Seismology, Earthquakes and Earth Structure, Blackwell Publishing.

UNDP, 1984, Exploration for diamonds (Phase I); Exploration for minerals (Phase II), Technical Report**;** *Geology and Mineral Resources of Lesotho*: Maseru, Department of Mines and Geology, Lesotho.

www.geoscience.org.za

www.ciw.edu/kaapvaal

www.isc.ac.uk